belspo

BRAIN-be
Belgian Research Action through Interdisciplinary Networks

PIONEER PROJECTS

LOCALIZED TIDAL HEATING ON ENCELADUS

CONTRACT - BR/314/PI/LOTIDE

FINAL REPORT

15/03/2017

Promotor
Michael Beuthe
Royal Observatory of Belgium
Reference Systems and Planetology
Avenue Circulaire 3 - B-1180 Brussels

Author
Michael Beuthe

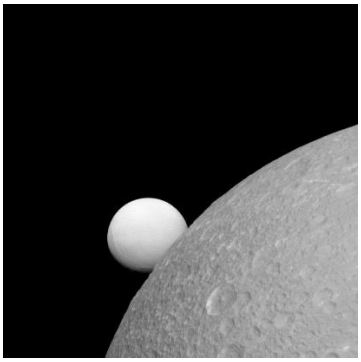

.be

Published in 2018 by the Belgian Science Policy
Avenue Louise 231
Louizalaan 231
B-1050 Brussels
Belgium
Tel: +32 (0)2 238 34 11 – Fax: +32 (0)2 230 59 12
http://www.belspo.be

Contact person: Georges JAMART
+32 (0)2 238 36 90

Michael Beuthe ***Localized Tidal Heating on Enceladus (LOTIDE)***. Final Report. Brussels : Belgian Science Policy 2017 – 34 p. (BRAIN-be - Belgian Research Action through Interdisciplinary Networks)

TABLE OF CONTENTS

SUMMARY

Context

Saturn's moon Enceladus is celebrated for its huge fractures venting jets of water vapor and ice particles at the south pole. From 2005 to 2015, numerous flybys by the spacecraft Cassini have provided incontrovertible evidence for an underground water reservoir beneath Enceladus' south polar terrain: more than one hundred water geysers are identified, ammonia along with various organic compounds and salt-rich ice grains are detected in the plume, silica nanoparticles point to hydrothermal activity, and weak gravity anomalies suggest buoyant support of the topography. Finally, measurements of large librations reveal in 2015 that this liquid layer forms a global ocean under a thin crust. Crustal thickness remains however a controversial subject because gravity data predicts instead a thick crust. Besides being geologically active, the south polar region is anomalously warm, emitting heat at a rate exceeding theoretical expectations by a factor of ten. The most likely source of heating at this scale comes from tidal dissipation but it is not clear where and how most of the energy is dissipated. Regarding the `where', dissipation can either occur through viscoelastic deformations in the crust and core, or result from dissipative tidal waves in the ocean. Wherever dissipation occurs, the power output is too small by one or two orders of magnitude. Regarding the `how', classical computations of dissipation neglect lateral variations of crustal thickness or rigidity, which must be large otherwise geological activity would be not be localized at the south pole. Explaining Enceladus's heat engine is a precondition to understand the long-term stability of the ocean and its suitability for extra-terrestrial life.

Objectives

The first objective of the LOTIDE project is to develop a new and faster method to compute tidal dissipation in small bodies with lateral heterogeneities, based on the modelling of the crust as a spherical thin shell with variable thickness or rigidity and having depth-dependent rheology. With this model, we propose to test the hypothesis that tidal dissipation is enhanced by the local extension and local bending of a thinner crust in the south polar region, and compare the predictions with the global heat flow extracted from Cassini data. In particular, we intend to couple heat production with conductive heat transport in order to see whether crustal dissipation accounts for the latitudinal variations in the surface heat flux. The second objective of LOTIDE consists in doing a new analysis of the gravity-topography data with the aim of determining the lateral variations of crustal thickness and reconciling these predictions with those of librations. The results will be used as an input for the tidal dissipation model in the first objective. The third objective of LOTIDE is to study whether oceanic tidal waves could significantly contribute to dissipation if the ocean is buried under an elastic crust. This goal requires the development of a new model of ocean tides including the damping effect of the crust.

Conclusions

Regarding the first objective, we successfully developed a new theory of tidal deformations and dissipation within a non-uniform viscoelastic shell which is mechanically and gravitationally coupled to a global ocean and a viscoelastic core. Moreover, we wrote a numerical code solving the non-uniform thin shell equations in the spectral domain, and evaluating the resulting dissipation. The code is fast and converges well even if the lateral variations of the shell properties have a large amplitude; it can be applied to local oceans as well. We coupled the code to conductive heat transport in order to generate self-consistent solution for tidal heating and crustal rheology. Using this code, we showed that the non-uniformity of the crust strongly increases heat flux variations across the surface of Enceladus. If dissipation in ice is as large as suggested by recent laboratory experiments, crustal dissipation could account for most variations of the surface heat flux. However, the crust cannot be the unique source of Enceladus's heat since the core contributes at least 50% of Enceladus's total heat output in order to maintain the crust in thermal equilibrium. The analysis of crustal dissipation above a local ocean demonstrates that the ocean needs to be global in order to let the crust and the core deform and dissipate. The non-uniform shell model will be used in the future to study simultaneous dissipation in crust and core, and can be coupled to dissipative ocean tides if needed. Therefore, the non-uniform thin shell approach will likely be an essential part of future models of tidal dissipation in Enceladus, as well as Europa which is the next target for a mission to an icy moon.
As for the second objective, we identified the reason why gravity-topography analysis and librational models led to different estimates for the crust thickness. The problem lies in the spherical isostasy approach used to relate gravity anomalies to topography, which breaks down at the largest scale. Accordingly, we developed a new approach to spherical isostasy based on self-consistent gravito-elastic equations and minimization of the crustal deviatoric stress. Applying this model to Enceladus, we showed that a correct gravity-topography analysis predicts the same thin crust (between 19 and 27 km thick on average) as estimated from librations. The crust is even thinner (3 to 11 km thick) at the south pole, facilitating the opening of water conduits and enhancing dissipation through stress concentration (see the first objective). Applying the same approach to Saturn's moon Dione resulted in a ground-breaking result: Dione harbors a deep ocean beneath a 100 km-thick crust. Our new isostatic model will become the new standard for large-scale isostasy in icy moons (Europa, Titan, Ganymede), large asteroids (Ceres), and terrestrial planets (Mercury, Venus, and Mars).

Regarding the last objective, we built the first model of dissipative tides in a subsurface ocean, by combining the Laplace Tidal Equations with the thin shell approach. For the first time, it is possible to compute tidal dissipation rates within the crust, ocean, and mantle in one go. We showed that the presence of the crust shifts the tidal resonances to smaller depths. As a result, oceanic dissipation is strongly reduced by the crustal constraint, and thus contributes little to Enceladus' present heat budget. Tidal resonances, however, could have played a role in the formation or the freezing of an ocean less than 100 m deep, and therefore act as a protection mechanism against freezing the whole satellite. Finally, we showed that crustal dissipation due to oceanic obliquity tides in a low viscosity ocean can differ from the static prediction by up to a factor of two.

Keywords

Enceladus

Dione

Solid tides

Oceanic tides

Tidal dissipation

Planetary dynamics

Icy satellites

Gravitational anomalies

Isostasy

RESUME

Contexte

Encelade, une lune de Saturne, est réputée à juste titre pour les énormes fractures traversant la région polaire australe, desquelles jaillissent des jets de vapeur d'eau et de particules de glace. De 2005 à 2015, de nombreux survols par la sonde spatiale Cassini ont révélé l'existence d'un réservoir d'eau souterrain au pôle sud: plus de cent geysers sont identifiés, de l'ammoniac ainsi que des composés organiques et des grains de glace riches en sel sont détectés dans le panache, la détection de nanoparticules de silice indique une activité hydrothermale, et les faibles anomalies gravitationnelles suggèrent que la topographie de surface est maintenue par la poussée d'Archimède comme un iceberg flottant sur l'eau. Finalement, la mesure de librations de grande amplitude montre en 2015 que la couche liquide forme un océan global sous une croûte mince. La détermination de l'épaisseur de croûte reste cependant sujette à débat puisque les données gravitationnelles prédisent plutôt une croûte épaisse. En plus d'être géologiquement active, la région polaire australe est anormalement chaude, émettant un flux thermique bien au-delà des prédictions théoriques. La source la plus probable de chaleur à cette échelle est la dissipation due aux marées, mais nous ne savons pas encore où ni comment la majeure partie de l'énergie est dissipée. Concernant la question du "où", la dissipation peut se produire en raison des déformations viscoélastiques dans la croûte et le noyau, ou alors résulter d'ondes de marées dissipatives à l'intérieur de l'océan. Quel que soit l'endroit où la dissipation se produit, la puissance résultante est trop petite d'un ou de deux ordres de grandeur. Concernant la question du "comment", les calculs classiques de dissipation négligent les variations latérales de l'épaisseur de la croûte ou de sa rigidité, qui doivent être importantes sinon l'activité géologique ne serait pas limitée au pôle sud.

Objectifs

Le premier objectif du projet LOTIDE est de développer une nouvelle méthode rapide pour calculer la dissipation de marée dans des petits corps possédant des hétérogénéités latérales importantes. Cette méthode se base sur la représentation de la croûte par une coquille sphérique mince ayant une épaisseur et une rigidité variables, ainsi qu'une rhéologie dépendant de la profondeur. Grâce à ce modèle, nous allons tester l'hypothèse que la dissipation de marée est accrue en raison de l'extension et déflexion locales d'une croûte amincie au pôle sud. Nous comparerons les prédictions du modèle avec le flux thermique de surface mesuré par la sonde Cassini. En particulier, nous lierons la production de chaleur au transport conductif de chaleur de façon à vérifier si la dissipation à l'intérieur de la croûte est la cause des variations en latitude du flux thermique. Le second objectif de LOTIDE consiste en une nouvelle analyse des données gravitationnelles et topographiques en vue de déterminer les variations latérales de l'épaisseur de croûte et réconcilier ces prédictions avec celles des librations. Ces résultats seront utilisés dans le modèle de dissipation de marée du premier objectif. Le troisième objectif de LOTIDE est de déterminer si les ondes de marée océaniques peuvent contribuer de manière significative à la dissipation totale dans le cas réaliste où l'océan gît sous une croûte élastique. L'accomplissement de cet objectif nécessite le développement d'un nouveau modèle de marées océaniques tenant compte de l'effet d'amortissement de la croûte.

Conclusions

Concernant le premier objectif, nous avons développé avec succès une nouvelle théorie des déformations de marée et de la dissipation à l'intérieur d'une coquille mince viscoélastique qui est couplée mécaniquement et gravitationnellement à un océan global et à un noyau viscoélastique. De plus, nous avons écrit un programme résolvant numériquement les équations de la coquille mince dans le domaine spectral, et calculant la dissipation associée. Le programme est rapide et converge bien même si les variations latérales des propriétés de la coquille sont de grande amplitude; le programme s'applique aussi aux océans d'extension limitée. Nous avons couplé le programme au transport de chaleur conductif en vue de générer une solution cohérent pour le chauffage de marée et la rhéologie de la croûte. Grâce ce code, nous avons montré que la non-uniformité de la croûte augmente fortement les variations en latitude du flux thermique à la surface d'Encelade. A supposer que la dissipation dans la glace est aussi grande que celle estimée dans de nouvelles expériences de laboratoire, la dissipation dans la croûte pourrait être la cause de la majeure partie des variations du flux thermique à la surface. Cependant, la croûte ne peut pas être la seule source de chaleur puisque le noyau doit fournir au moins la moitié de la puissance totale pour maintenir l'équilibre thermique de la croûte. Par ailleurs, l'analyse de la dissipation dans la croûte au-dessus d'un océan d'extension limitée montre que l'océan doit être global de manière à laisser la croûte et le noyau se déformer et dissiper de l'énergie. Dans le futur, le modèle de coquille non-uniforme sera utilisé pour étudier la dissipation simultanée dans la croûte et le noyau, et pourra être couplé aux ondes de marée océaniques si nécessaire. En conclusion, le modèle de coquille mince non-uniforme fera sans doute partie de tous les nouveaux modèles de dissipation de marée pour Encelade ainsi que pour Europe (le satellite de Jupiter) qui est la prochaine cible d'une mission spatiale vers un satellite de glace.

Concernant le second objectif, nous avons identifié la raison pour laquelle l'analyse des données gravitationnelles et topographiques et des mesures de libration menaient à des estimations différentes de l'épaisseur de croûte. Le problème réside dans la théorie d'isostasie sphérique utilisée pour relier les anomalies de gravité à la topographie. Cette théorie n'est plus correcte à grande échelle. Par conséquent, nous avons élaboré une nouvelle théorie de l'isostasie sphérique basée sur les équations gravito-élastiques et la minimisation des tensions déviatoriques dans la croûte. En appliquant cette méthode à Encelade, nous avons montré qu'une analyse correcte des données gravitationnelles et topographiques prédit la même épaisseur de croûte (entre 19 et 27 km en moyenne) que celle estimée à partir de la libration. La croûte est amincie au pôle sud (3 à 11 km d'épaisseur), facilitant donc le passage de l'eau souterraine vers la surface et augmentant la dissipation en raison de la concentration des tensions (voir le premier objectif). L'application de la même méthode à Dioné, une autre lune de Saturne, a mené à une conclusion remarquable: Dioné possède un océan profond sous une croûte de 100 km d'épaisseur. Notre nouvelle théorie isostasique est en passe de devenir la référence pour l'isostasie à grande échelle dans les satellites de glace (Europe, Titan, Ganymède), l'astéroïde Cérès et les planètes telluriques (Mercure, Vénus et Mars).

Concernant le dernier objectif, nous avons construit le premier modèle d'ondes de marée dissipatives dans un océan souterrain, en combinant les équations de marée de Laplace avec la théorie des coquilles minces. Il est maintenant possible de calculer simultanément la dissipation de marée dans la croûte, l'océan et le manteau. Nous avons montré que la présence de la croûte déplace les résonances de marée vers des profondeurs océaniques plus petites. Par conséquent, la dissipation océanique est fortement diminuée par la contrainte de la croûte, et contribue donc peu à la puissance thermique totale d'Encelade. Cependant, les résonances de marée pourraient avoir joué un rôle dans la formation ou la disparition d'un océan de moins de cent mètres de profondeur, et agissent donc comme un mécanisme de

protection contre la solidification complète du satellite. Finalement, nous avons montré que la dissipation dans la croûte due aux marées océaniques d'obliquité dans un océan de faible viscosité pourrait être deux fois plus petites que la prédiction de la théorie des marées statiques.

Mots-clés

Encelade

Dioné

Marées solides

Marées océaniques

Dissipation de marée

Dynamique planétaire

Satellites de glace

Anomalies gravitationnelles

Isostasie

1. INTRODUCTION

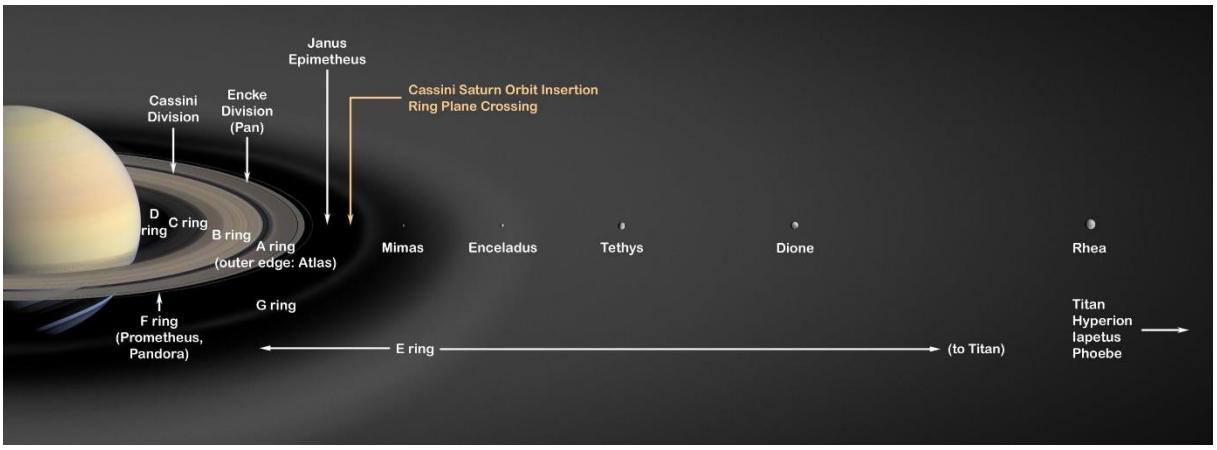

Figure 1: Saturn's rings and its five mid-size icy moons between the rings and the giant moon Titan. Saturn's diffuse E ring is the largest planetary ring in our solar system, extending from Mimas' orbit to Titan's orbit, about 1 million kilometres. The particles in Saturn's rings are composed primarily of water ice and range in size from microns to tens of meters (Image PIA03550, credit: NASA/JPL).

For nearly two centuries after its discovery by William Herschel in 1789, Saturn's moon Enceladus remained nearly anonymous among the five mid-size satellites between the main ring system and the gigantic moon Titan (Figure 1). Though astronomers suspected in the 1980s that the remarkably bright Enceladus could be the source of Saturn's outer E ring, definitive proof had to wait until the arrival in 2004 of the Cassini spacecraft in the Saturn system (Spahn et al, 2006). In the first year of Cassini's operations, high resolution pictures show that the south pole area of Enceladus is completely disrupted by recent geologic activity (Porco et al., 2006). Four long parallel cracks crossing the polar region, nicknamed `tiger stripes', emit jets that form a plume of water vapor and icy particles above the south pole (Figure 2). Furthermore, the infrared instrument measures several gigawatts of thermal emission with highest temperatures along the tiger stripes (Spencer et al., 2006). Enceladus becomes the first known icy world with deep-seated geologic activity.

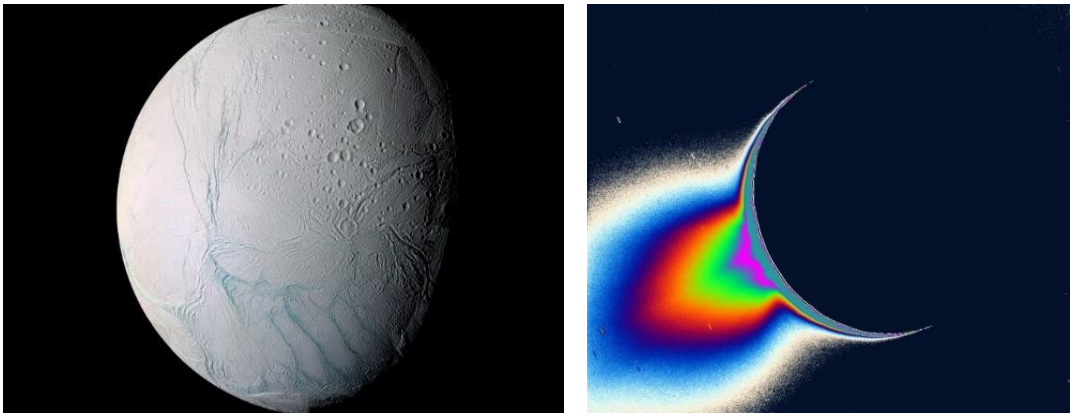

Figure 2: Left: global view of Enceladus taken by Cassini in 2005, with the four tiger stripes visible (in blue) at the bottom of the picture (Image PIA06254). Right: Enhanced and colorized image of the plume of Enceladus backlit by the Sun, taken by Cassini in 2006 (Image PIA07759). Credit: NASA/JPL/Space Science Institute.

From 2005 to 2015, 23 flybys - some as close as 25 km from the surface - generated a wealth of data. In particular, the jets have been traced to hotspots associated with the warmest parts of the tiger stripes (Spitale et al., 2007; Porco et al, 2014). The presence of ammonia in the plume (Waite et al., 2009) and of salt in the emitted icy particles (Postberg et al., 2009; 2011) revealed the existence of a subsurface reservoir of liquid water, while the detection of silica nanoparticles in the E ring (Hsu et al, 2015) points to hydrothermal activity on the ocean floor. Two questions immediately arise: is the reservoir only located at the south pole, and at which depth is it buried? At first, the comparison of gravity and topography data was interpreted in terms of a local underground sea under the south pole (Figure 3), at a depth of 30-40 km (Iess et al., 2014). Further analysis suggested that the reservoir was global and buried under a 50 km-thick crust (McKinnon, 2015), but this estimate was hardly compatible with water eruptions at the south pole and left little room for an ocean between crust and core. At the start of the LOTIDE project in early 2015, not much was understood about Enceladus's ocean: was it local or global, and was it buried under thick or thin ice? In late 2015, the measurement of large librations breaks the tie: the crust is decoupled from the core by a global ocean (Thomas et al, 2016). The amplitude of librations however indicates that the crust is less than 26 km thick, in conflict with the 50 km value predicted by gravity-topography analysis. We will go back to this issue which is important for our project.

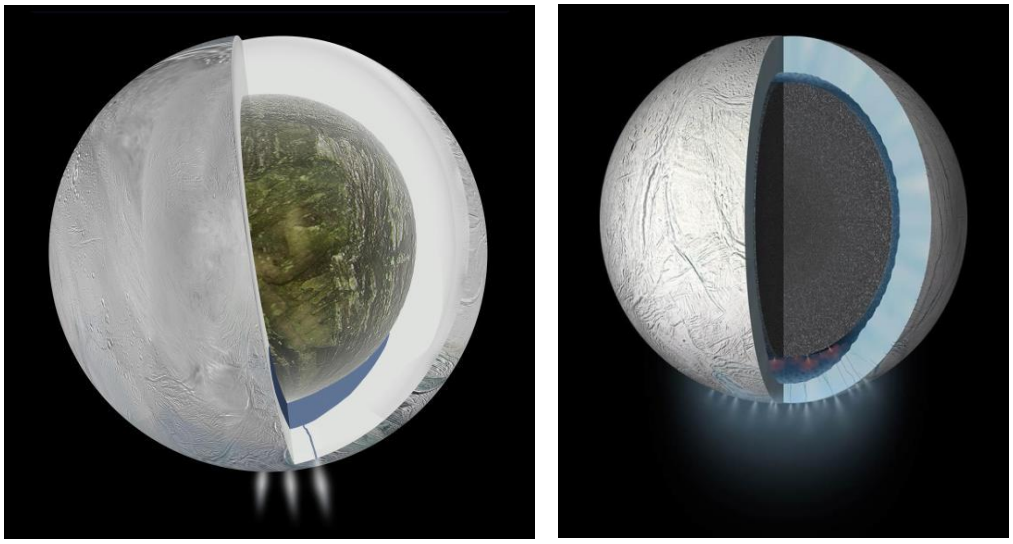

Figure 3: Left: possible interior structure of Enceladus inferred from the gravity-topography data by Iess et al (2014), with a local ocean at the south pole (Image PIA18071). Right: possible interior structure of Enceladus inferred from the same data by McKinnon (2015), with a global ocean under a thick crust (Image PIA20013). Credit: NASA/JPL-Caltech.

Notwithstanding the numerous flybys, estimates of Enceladus' heat output are still very uncertain. The initial estimate of 4 to 8 GW, from high-temperature emission (Spencer et al., 2006) was later revised upward to 13-19 GW by including lower-temperature emission (Howett et al., 2011). High-resolution scans however implied that the tiger stripes alone emitted only 4 GW (Spencer et al., 2013). Observations made during two late 2015 flybys suggest that significant thermal emission occurs between the tiger stripes (Spencer et al., 2016), but numerical estimates have not yet been published (as of March 2017). Whatever the precise value of the power output, the above estimates are much higher than theoretical predictions based either on interior thermal modelling or on dissipative equilibrium with Saturn (see below).

Our research project addresses the question of the heat engine behind the geologic activity on Enceladus. At the present day, neither internal radioactivity nor chemical reactions provide enough energy (Malamud and Prialnik, 2013; Travis and Schubert, 2015) but tidal forces (due to the non-circular orbit) can generate high rates of dissipation, as demonstrated by the volcanism on Jupiter's moon Io. In support of this explanation, Enceladus' plume is brighter at the apocenter of the orbit when tidal forces tend to open the tiger crack, although the timing of individual jets appears to be random (Hedman et al., 2013; Nimmo et al, 2014). In principle, tidal heating can occur at all depths within the satellite but the core does not dissipate enough even if it is an aggregate of ice and silicates (Roberts, 2015). The most likely source of tidal heating arises from deformations and friction in the crust (Hurford et al., 2007; Nimmo et al., 2007). Shear friction along fault lines has now been shown to be incompatible with observations (Nimmo et al., 2014), but tidal dissipation could arise from viscoelastic deformations of the whole crust. However, this mechanism has its own problems. In present models, the power output is too small (by up to a factor 10) and the heat transport to the surface is too efficient, resulting in the freezing of the subsurface ocean and the end of the high-dissipation regime (Roberts and Nimmo, 2008; Tobie et al., 2008; Behounkova et al., 2012). Changing the rheology of ice does not solve the problem (Behounkova et al., 2013; Shoji et al., 2013) while adding anti-freeze agents such as ammonia to the ocean only slows down the freezing (Roberts and Nimmo, 2008; Tobie et al., 2008).

One possible solution to the heating problem is to postulate that Enceladus is now in a transient regime in which the dissipated energy is the leftover from an orbital state of higher eccentricity and higher dissipation (O'Neill and Nimmo, 2010; Shoji et al, 2014). Episodic heat production would mean that we observe Enceladus at a very special time. The active phase indeed only lasts a few millions years, with a dormancy period of the order of 100 million years. The difference in time scale between active and dormant phases results from the rapid decrease of the orbital eccentricity when the body dissipates a lot, whereas the eccentricity increases very slowly when dissipation is low. There is thus a low a priori probability that our observations coincide with Enceladus being at the end of its active phase, when the eccentricity has fallen to a low level but the icy shell is still warm. While episodic heating was favored by previous estimates of dissipation within Saturn (Meyer and Wisdom, 2007), recent analysis of astrometry data suggests that dissipation within Saturn - and thus also within Enceladus - is higher by an order of magnitude (Lainey et al., 2012; 2017). We will thus study in this project alternative solutions to the problem of `too little heat/freezing ocean'.

Classical computations of tidal dissipation are based on an approach designed for much larger satellites such as Europa, where gravity dominates elastic effects (the crust follows the deformation of the ocean) so that tidal deformations are not much affected by lateral crustal inhomogeneities. In that case, dissipation is mostly due to viscoelastic lateral extension/compression of the crust of harmonic degree two, with very little contribution from bending or twisting. This approach has been applied to Enceladus by several groups (Ross and Schubert, 1989; Barr, 2008; Roberts and Nimmo, 2008; Han et al., 2012; Shoji et al., 2013; 2014; Rozel et al., 2014). However, Enceladus is small (252 km radius, a sixth of Europa's size) and its surface gravity is weak (0.1 m/s^2, less than a tenth of Europa's gravity) so that elasticity dominates gravity.
The geologic activity present at the south pole but not elsewhere suggests strong spatial variations of the crustal rigidity. Besides, gravity/topography analysis predicts large variations in crustal thickness (Iess et al, 2014; McKinnon, 2015). We thus expect that tidal deformations have components of harmonic degrees other than two and that local viscoelastic effects with bending/twisting give a significant contribution to tidal heating. To date, there is only one model that self-consistently computes tidal dissipation in a three-dimensional viscoelastic body (Behounkova et al., 2010; 2012; 2013), but it was specifically developed for bodies with thick convecting crusts whereas librations suggest that Enceladus has a thin conductive crust.

Moreover, its complexity makes it difficult to examine all physically interesting cases. The main thrust of our project will thus be the development of a new model of tidal deformations in a non-uniform crust which is based on thin shell theory.

At the start of the project, Cassini data did not favor a global ocean over a local sea (Collins and Goodman, 2007), but the situation soon changed once librational data became available. It was thus logical to investigate in more detail the global sea solution. In that regard, the question of the crustal thickness became crucial: gravity-topography analysis was necessary to provide the crustal thickness variations used in our model of tidal deformations, but its estimate of the mean thickness was incompatible with librational data. We have added this question to the LOTIDE project. Finally, the fact that Enceladus's ocean is global gives a new chance to a more exotic scenario for tidal dissipation, in which anomalous heating arises from dissipative ocean tides (Tyler, 2011; 2014; Matsuyama 2014). Ocean tides exhibit interesting resonant behaviour which enhances the tidal deformation and dissipation. Existing models, however, studied Enceladus's ocean tides as if they occurred in a surface ocean. The thin shell approach being ideally suited to this problem, we added to the LOTIDE project an investigation of dissipation in subsurface ocean tides.

In summary, the objectives of the LOTIDE project are:

- to develop a new and faster method to compute tidal dissipation in small bodies with lateral heterogeneities, based on the modelling of the crust as a 2D spherical shell with variable thickness or rigidity and with depth-dependent rheology,
- to test the hypothesis that tidal dissipation is enhanced by local extension and local bending of a thinner crust in the south polar region, and compare the results with the global heat flow extracted from Cassini data,
- to couple heat production with conductive and convective heat transport, in order to see whether crustal dissipation accounts for spatial variations in the surface heat flux.
- to determine the variations in crustal thickness by a new analysis of gravity-topography data,
- to study whether subsurface ocean tides could significantly contribute to dissipation.

2. METHODOLOGY AND RESULTS

Thin shell theory with non-uniform viscoelasticity

Tidal dissipation inside the crust occurs because the crust is viscoelastic. This property varies a lot with depth, from the very hard surface exposed to space to the near-melted ice at the crust-ocean boundary. Moreover, the rigidity and viscosity of the crust must vary a lot with latitude, since Cassini detected anomalous heating at the south pole of Enceladus, but not elsewhere. Besides, the standard theory of tidal heating predicts strong variations in the intensity of dissipation between the equator and the poles, on the one hand, and between the tidal axis and the tangent to the orbit, on the other. It is thus essential to develop an approach in which one can compute the viscoelastic deformations of a completely non-uniform crust.

As a starting point, we used the thin elastic shell theory of Beuthe (2008; 2010) describing the deformations of a thin elastic shell with non-uniform rigidity. Our three aims regarding this theory were to extend it from elastic shells to viscoelastic shells, to include the depth-dependent properties of the crust, and to couple it to tidal forcing. Including radial inhomogeneities is more difficult than in membrane theory (Beuthe 2015a; 2015b), since it requires to reformulate thin shell theory so that the middle surface of the shell loses its privileged status. This formalism leads to a new coordinate-invariant definition of the effective bending rigidity of the shell, which is equivalent to the classical formula of the bending rigidity

when the properties of the shell do not depend on depth. The new theory takes the neat form of two governing equations which are partial differential equations of the fourth order in derivatives and scalar in spherical coordinates. The sought-for functions are the radial deflection of the shell and the generating function for the stresses. The consistency of the result is guaranteed by two symmetries: first, the governing equations satisfy static-geometric duality (as they should) and second, they do not depend - at leading order in shell thickness - on the choice of the shell reference surface. The next-to-leading dependence on the reference surface is minimized by choosing shell coordinates such that the first moment of the shear modulus vanishes.
Coupling to tidal forcing is a delicate matter because of the self-gravity problem: while Saturnus's tidal potential deforms Enceladus, the deformation of Enceladus itself changes the total external gravitational potential. This well-known feedback effect must be taken into account in any self-consistent theory of gravitational deformation. We used an original approach to treat the case of a fully viscoelastic satellite: it consists in modelling the action of the crust on the ocean through pressure Love numbers, which are then related to the better-known tidal Love numbers of the satellite. After tidal coupling, the governing equations of the thin shell depend on Saturnus's tidal potential and on the so-called fluid-crust tidal Love numbers of Enceladus, which depend on the density structure of the core and ocean, and on the viscoelasticity of the core. Note that the model allows us to compute dissipation in the core. The non-uniform thin shell theory of viscoelastic tidal deformations is now complete.
Next, we must evaluate the tidal dissipation produced by the dephasing of microscopic stress and strain throughout the whole crust. Instead of integrating on the product of stress and strain at each point, we adopted the following innovative approach: the dissipated power is directly expressed in terms of the deflection and the stress generating function with the help of a spherical differential operator of the fourth order. Computing dissipation in this way is more accurate and much faster: no tensorial products are involved because only scalar quantities are involved. This formulation has also the advantage of keeping separate the contributions to dissipation of membrane and bending stresses (with a third term resulting from mixing between the two). We are finally able to predict the heating rate at all points within the non-uniform crust, the resulting surface flux, and the total power dissipated by tides.

LOTIDE software development

If the satellite has a spherically symmetric internal structure, the equations governing the tidal deformations are linear with constant coefficients in the spatial domain, which makes them easy to solve in the spectral domain where they are diagonal. Here, the strongly asymmetric structure of the crust implies that the coefficients of the partial differential equations are not constant in the spatial domain; in the spectral domain, it introduces couplings between the spectral deformational modes. A first option consists in working in the spatial domain and solving the partial differential equations with a finite difference method. This approach, however, presents difficulties due to the apparent singularities of spherical coordinate systems and the cancelling of the translation degree of freedom in thin shell theory (harmonic degree one). The second option, which we adopted here, consists in solving in the spectral domain a truncated system of linear equations coupled by means of Wigner 3-j symbols: the solution is then obtained by standard matrix manipulations. The size of the system depends on the cut-off spectral degree, determined by the scale of the lateral variations in crustal properties.

For this purpose, we have written LOTIDE.f90, a FORTRAN code solving for the viscoelastic deformations of the thin shell and the generating function for the stresses. Transformations between the spatial and spectral domain are done with the external library SHTOOLS (Wieczorek et al, 2016), while matrix manipulations are done with the linear algebra package LAPACK. The couplings between equations depend on the spatially-dependent membrane and bending rigidities. Given the viscoelastic properties and the geometry of the shell, the code

computes the deflection of the shell as well as the associated stresses. The code is fast and converges well, even if the lateral variations of the shell properties have a large amplitude. As a preliminary step, we benchmarked the FORTRAN code for the tidal deformation of a shell with uniform properties, for which the solution is well-known. Next, we tested the code for an interior model of Enceladus with a global ocean and a laterally non-uniform shell, similar to the one proposed by Behounkova et al. (2015). Deformations and stresses are enhanced in the south polar area where the crust is thinner and softer. The case of a local ocean can be modelled it by imposing that the crust is extremely rigid, except in the southern area where the subsurface ocean is present (imposing a tangential load, as considered in the proposal, is problematic because it must be iteratively adjusted at every point on the shell). It is possible to use the code already developed for a global ocean case with a few modifications. We tested the convergence of the resulting code for very strong lateral variations of the rigidity which are required in this case. The code converges well if the cut-off degree of the spectral expansion is high enough.

In the second stage of the LOTIDE software development, we implemented our new method for evaluating the dissipated energy in terms of the deformations and the generating stress function provided by the first part of the program. The spherical differential operator yielding the dissipated energy is evaluated in an efficient way via pseudo-spectral transforms. The contributions of membrane and bending stresses are kept separate in the output. We benchmarked the dissipation part of the code by computing the spatial patterns of tidal heating at all depths within a laterally uniform conductive crust, which has a soft rheology close to the crust-ocean boundary. These heating patterns closely follow those predicted by thick shell theory (Beuthe 2013). Besides, we applied the code to the case already used to test the deformation part of the code. Dissipation is enhanced in the south polar area where the crust is softer. If the crust is locally thinner, the total dissipated power is higher though the dissipation volume is smaller, because stresses and strains are much larger.
In the third stage of LOTIDE software development, we coupled the deformation-dissipation LOTIDE code to conductive heat transport. In the conductive heat equation, the heating rate due to tidal dissipation appears as a source term whose magnitude varies from high at the bottom of the crust to low near the surface. We solve the heat equation for the crustal temperature profile with the BVP solver for boundary value ordinary differential equations {Shampine et al, 2006). As an input, the heat equation requires knowing the dissipation within the crust. However, dissipation depends (through crustal rheology) on the temperature profile of the crust. We thus initiate the program by neglecting the influence of tidal dissipation when solving for the temperature profile. Next, we compute the dissipated power corresponding to this rheology, before solving again the heat equation with dissipation as a source term. We then iterate these two steps several times until the value of the dissipated power stabilizes. At each iteration, we determinate anew the shell coordinates minimizing the next-to-leading corrections to the thin shell equations.

Coupling to convective heat transport was not developed as far as the coupling to conductive heat transport. While we can compute the tidal dissipation given the rheology of the convecting crust, we did not try to determine the influence of tidal dissipation on convection itself for two reasons. First, parameterized convection has only been benchmarked for layers of uniform thickness, whereas Enceladus's crust thickness varies by a factor of 4 between the south pole and the equator. Second, convection simulations indicate that convection does not occur if Enceladus's crust is thinner than 40 km (Barr and McKinnon, 2007; Mitri and Showman, 2008).

Dissipation in a non-uniform crust: results

In the case of a global ocean, the reference model for the structure of the crust is provided by our isostatic analysis of the gravity-topography data, except that we neglect the rather modest longitudinal variation in crustal thickness: the crust varies from 29 km at the equator to 14 km and 7 km at the north and south pole, respectively (Figure 4), with a mean thickness of 23 km. The surface temperature varies from 60 K at the poles to 80 K at the equator (Roberts and Nimmo, 2008). The temperature at the crust-ocean boundary is the melting temperature of ice (273 K). The viscosity of ice is related to temperature by an Arrhenius relation (Kirk and Stevenson, 1987). We assume that the rheology is of Maxwell type and that the viscosity at the melting temperature is 10^{13} Pa.s. The total power dissipated in the crust is 1.3 GW, 20% higher than the power dissipated in a uniform crust with the same mean thickness. The bending contribution to dissipation is moderate, about 7% of the total power. The power dissipated in the crust is not at all sufficient to maintain thermal equilibrium, being only 4% of the total conductive heat flux required to maintain the crust at the given thickness. While the non-uniform shell model does not yield a significant enhancement of the total power, it predicts much larger equator-to-pole heating rate variations (Figures 5 and 6). In particular, the surface flux resulting from crustal dissipation at the south pole increases by nearly a factor of 3 (reaching 7 mW/m^2) in comparison with the uniform thickness model (Figure 5B). However, most of the variation of the total surface flux must be explained by a variation in the heat flux coming from below at the crust-ocean boundary.

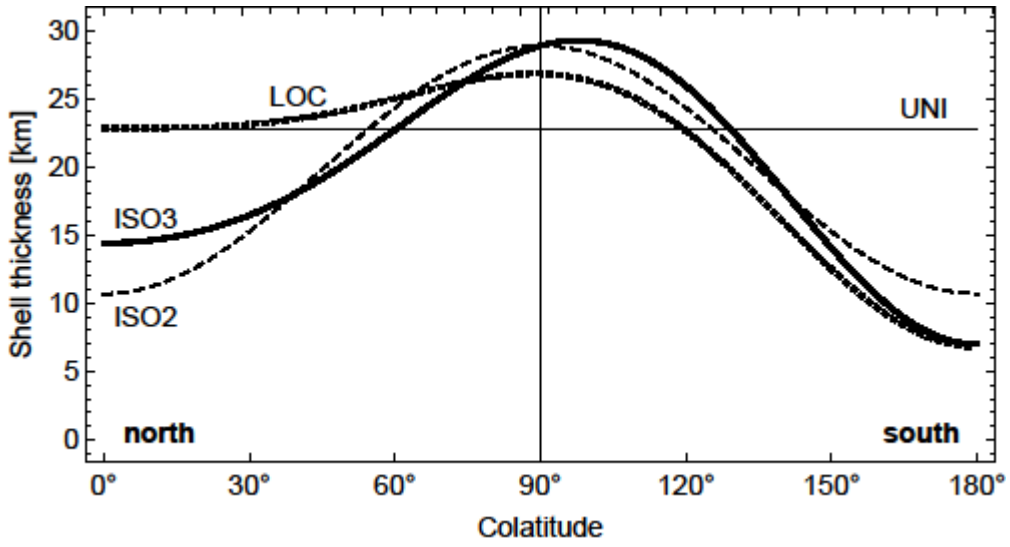

Figure 4: North-south variation of shell thickness (zonal average): ISO3 is the isostatic profile up to degree ~ 3 (solid curve), ISO2 is the isostatic profile up to degree ~ 2 (dashed curve), UNI is the 22.8 km-thick uniform profile, LOC is a made-up profile with thinning mostly located at the south pole (dotted curve).

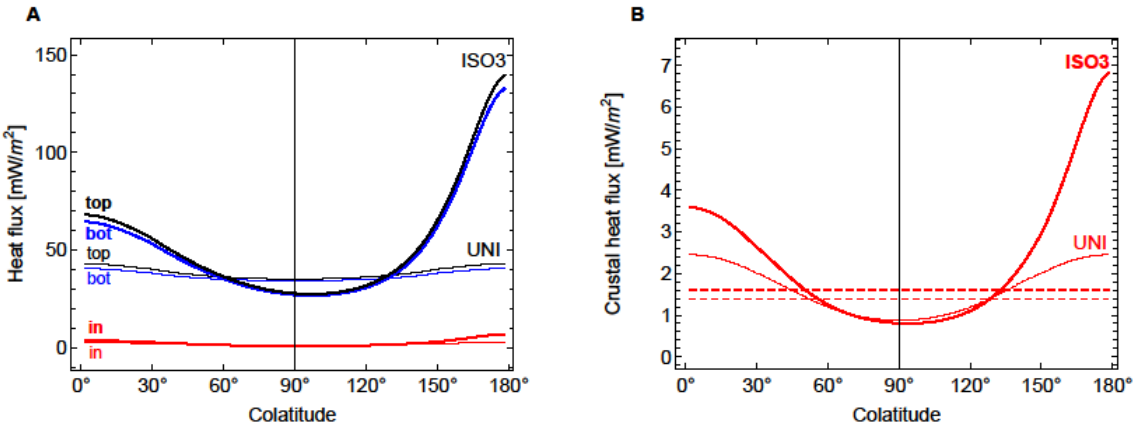

Figure 5: Crustal heat budget: (A) heat flux at the surface of the crust (`top'), coming from below the crust (`bot'), and produced within the crust (`crust'). Thick (resp. thin) curves show the results for the crustal thickness profile ISO3 (resp. UNI). (B) heat flux produced within the shell (blow-up of red curves in panel (A)). Horizontal dashed lines show the mean heat flux.

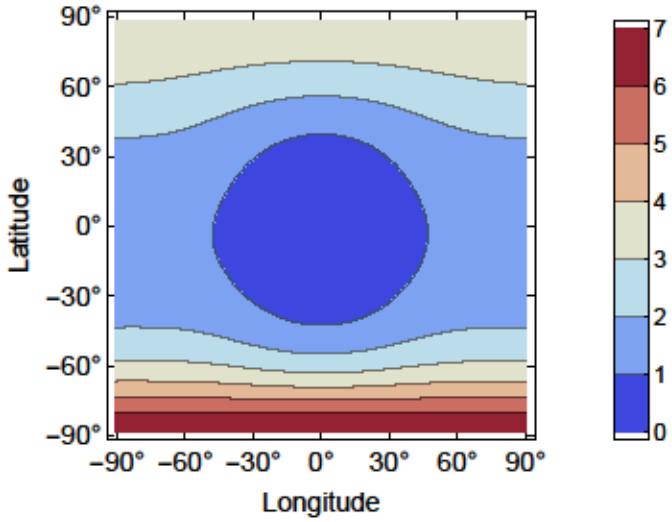

Figure 6: Spatial variations of the heat flux produced within the shell if crustal thickness is given by the model ISO3. The color scale is in mW/m^2. Longitude 0 corresponds to the tidal axis between Enceladus and Saturn. The pattern repeats itself between 90 degrees and 270 degrees.

Newly published laboratory studies of the anelastic response of ice at tidal frequencies suggest that dissipation could be an order of magnitude higher than predicted by the Maxwell model (McCarthy and Cooper, 2016). Since the corresponding rheological model is unknown, we choose to simulate this phenomenon by increasing Enceladus's eccentricity by a factor of about 3 (dissipation scales as the square of the eccentricity). The total power dissipated in the crust jumps to 16 GW, about 50% of the total power required to maintain the crust in thermal equilibrium. The bending contribution remains stable at 7%. In this model, the surface heat flux at the south pole reaches 150 mW/m^2, which is the central value measured by Spencer et al (2006). A remarkable feature of this model is that most of the surface flux variation is explained by the latitudinal variations of crustal dissipation, while the heat flux coming from below the crust varies much less (Figure 7A). By contrast, the uniform thickness model

completely fails to predict sufficient variations of the surface heat flux (Figure 7B). Interestingly, the heat flux coming from below the crust can be uniform in a model with no north-south asymmetry (Figure 7C). For completeness, we also considered a model in which there is no crustal thinning at the north pole, but it requires larger variations in the heat flux from below the crust (Figure 7D). We can draw the following conclusions about the non-uniform thickness model (assuming that the ocean is global):

- the total power dissipated in the crust moderately increases (by 10-20%).
- dissipation due to crustal bending is a minor contribution to the total power (7%).
- latitudinal variations in the surface flux are strongly enhanced (by a factor 2-3).
- under the assumption that dissipation in ice is an order of magnitude larger than in the Maxwell model, crustal dissipation contributes half of the total power and accounts for most of the latitudinal variations in the surface heat flux.

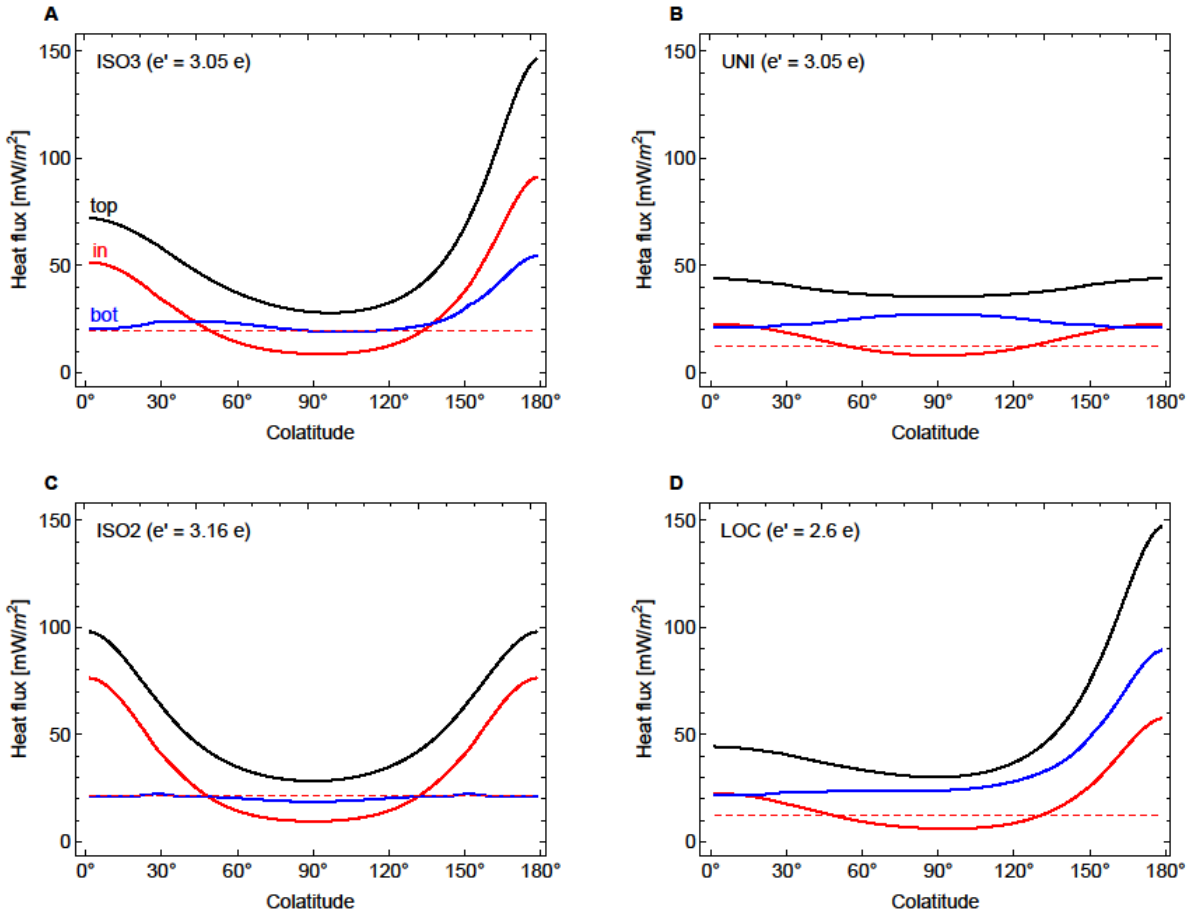

Figure 7: Crustal heat budget at higher eccentricity: heat flux at the surface of the crust (`top'), coming from below the crust (`bot'), and produced inside the crust (`in'). Horizontal dashed lines show the mean heat flux produced inside the crust. Panels (A), (B), (C), and (D) show the results for the thickness profiles ISO3, UNI, ISO2, and LOC, respectively.

Let us now consider the case of a local ocean. We assume that the ocean is centred at the south pole, has a total angular width of about 60 degrees and is buried beneath a 10 km-thick crust (mean value in the South Polar Terrain). In that model, dissipation is strongly localized in the South Polar Terrain, with a maximum at the ocean boundary where the crust undergoes most bending (Figure 8). Quantitatively, dissipation due to crustal bending contributes about 80% to the total power, showing that bending effects must be taken into account for local oceans. However, the surface flux is reduced by an order of magnitude (0.3-0.5 mW/m^2 in the

south pole area) in comparison with the case of a global ocean. This result is the nail in the coffin of the local sea model: while it has been guesses that it yielded too little power, no one had yet computed tidal dissipation in a thin shell above a local sea.

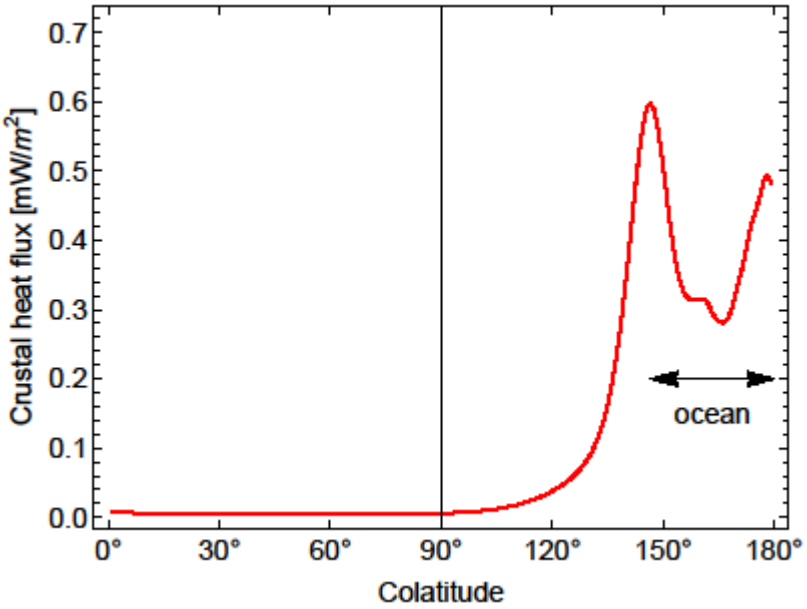

Figure 8: Heat flux produced within the shell in the model with a local ocean.

In conclusion, we have shown that using a non-uniform thin shell is essential to understand heat flux variations across the surface of Enceladus, but that the crust cannot be the unique source of Enceladus's heat: our results imply that the core contributes at least 50% of Enceladus's total heat output. In any case, the ocean needs to be global to let the crust and the core deform and dissipate. Since the non-uniform thin shell is coupled to a viscoelastic core, it can be used in the future to study simultaneous dissipation in the crust and in the core. If necessary, it is even possible to couple the non-uniform shell to dissipative ocean tides.

Enceladus's crust thickness from minimum stress isostasy

Variations in crust thickness can be inferred from their gravitational effect on the trajectory of the Cassini spacecraft during close flybys. Determining the mean crustal thickness is actually more difficult: it requires a mechanical model telling us how the surface topography is supported by the crust and how it is balanced by subsurface density anomalies. The first step consists in measuring how much Enceladus deviates from the hydrostatic ellipsoid shape. Using the shape and gravity data of Cassini (Nimmo et al, 2011; Thomas et al, 2016) and taking into account second-order corrections, we conclude that the observed shape and gravity of Enceladus deviate from hydrostaticity by thirty and ten percent, respectively. Such differences between the non-hydrostatic components of shape and gravity are indicative of isostasy, in which surface topography is mechanically supported and gravitationally compensated by a subsurface mass anomaly in such a way that below a certain depth, called the compensation depth, pressure is everywhere hydrostatic. Enceladus' degree-three zonal gravity harmonic (J3) also points to isostasy: it is only a third of what is expected from the corresponding shape harmonic. Degree-three compensation is attributed to isostatic support of the south polar depression (Iess et al, 2014).

Isostasy can occur either through crustal density variations (Pratt) or through variations in crustal thickness (Airy). For Pratt isostasy, the only plausible scenario involves porosity variations close to the surface, but compensation is too high (McKinnon 2015). With Airy isostasy, Enceladus' icy crust was initially estimated to be on average 30 to 40 km thick (Iess et al 2014), but this value was revised to 50 km due to second-order tidal-rotational effects (McKinnon 2015). A thick crust is hardly compatible with the south polar activity (Rudolph and Manga 2009), raises the issue of crust-core contact at the equator precluding isostasy, and does not match degree-three compensation (McKinnon 2015). Furthermore, the result conflicts with libration models predicting that the crust is half as thick (Thomas et al, 2016; Van Hoolst et al, 2016). The easy way out is to suppose that an elastic lithosphere partly supports the load (flexural isostasy) so that the subsurface mass anomaly can be smaller and located closer to the surface. Flexural support of long-wavelength loads, however, generates stresses that are not only larger than the tensional strength of intact ice but also much above the Coulomb failure criterion for a pervasively cracked thin lithosphere (McKinnon 2013). Cadek et al (2016) nevertheless argued for partial support of Enceladus' topography by a thin lithosphere, but ignore the problem of lithospheric failure.

Classical isostasy is an old but controversial subject. At the longest wavelengths, various isostatic prescriptions lead to geoid anomalies differing by more than a factor of two (Dahlen 1982). This question has never been settled because of the complexity of large-scale isostasy on Earth: thermal (Pratt) and Airy isostasy are dominant in oceanic and continental crusts, respectively, while the long-wavelength geoid is explained by mantle convection. In planetology, isostasy invariably resorts to the equal-mass prescription applied to conical columns (Lambeck 1988). This prescription however neither takes into account horizontal stresses nor geoid perturbations due to the loads themselves. Here we consider instead, following Jeffreys (1970) and Dahlen (1982), that the only physically meaningful isostatic prescription consists in minimizing crustal deviatoric stress in a self-consistent elastic-gravitational theory. Our approach is however very innovative in its use of Love numbers which encapsulate all the complications related to interior structure modelling.

The principle of minimum stress isostasy is based on the idea that, over time, the crust has reached the state of minimum deviatoric stress compatible with the observed topography through internal deformation, lithospheric failure and viscoelastic relaxation. In order to minimize crustal stresses, we need to know the deformations, gravity field perturbations, and stresses due to loads acting on the top and bottom of the crust. In terms of standard geophysical techniques, this means computing the elastic Love numbers of a self-gravitating spherically symmetric body submitted on the one hand to a surface load and, on the other, to an internal load located at the crust-ocean boundary (Greff-Lefftz et al, 2010). The two solutions are linearly combined with an arbitrary loading ratio, which is then fixed by minimizing the second invariant of the deviatoric stress tensor. We solve the elastic-gravitational problem with the incompressible propagator matrix method (Sabadini and Vermeersen, 2004). The surface and internal loads are modelled as thin layers at the surface and at the crust-ocean boundary. respectively. The final step consists in imposing the condition of minimum stress. For each harmonic degree, we minimize the total shear energy of the crust, which depends quadratically on crustal deformations. This constraint gives us a relation between the surface and internal loads, and thus determines the relief of the crust-ocean boundary in terms of the surface topography.

The determination of interior model parameters from data is an inverse problem which is nonlinear, under- or overconstrained depending on the parameter, and based on uncertain gravity and shape data. It is thus well suited to a Bayesian inference method (Sambridge 2011). The result of the Bayesian inversion is the posterior probability density function, i.e. the conditional probability for the parameters given the data (Gregory 2005). We simulate the

posterior probability density function with a Metropolis-Hastings sampler. From the generated samples, we compute for each parameter the probability density function, the mean value and the Bayesian confidence intervals of the interior model parameters.

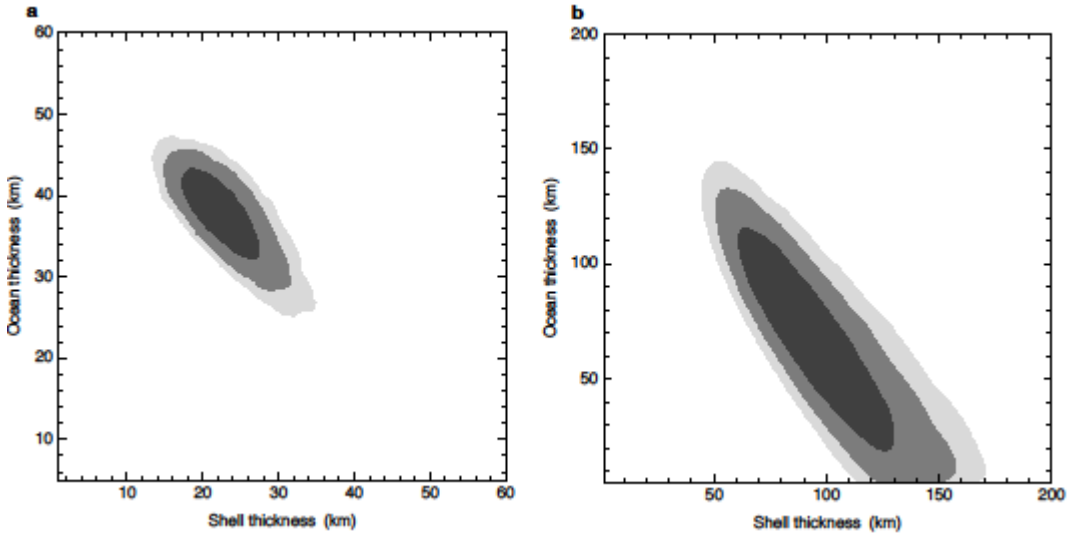

Figure 9: Inferred crust and ocean thicknesses: (a) Enceladus, (b) Dione. Contours show Bayesian confidence regions to (1σ, 2σ, 3σ). The ranges on the axes correspond to the prior uniform distributions. The inverse correlation between crust and ocean thicknesses is clearly visible.

At the long wavelengths, minimum stress isostasy requires a crust nearly half as thick as in classical isostasy. The Bayesian inversion for Enceladus yields a crust thickness of 23+-4 km (see Table I for the other parameters). Crust and ocean densities are not constrained. The crust and ocean thicknesses are inversely correlated (Figure 9a) because the core radius is well determined. Our estimates for Enceladus' crust thickness overlap with those of librations 21-26 km in Thomas et al (2016), 14-26 km in Van Hoolst et al (2016). For a rigorous comparison, we compute the librations from the probability distribution over the parameters inferred from our gravity-shape inversion assuming a rigid crust with non-hydrostatic boundaries (Van Hoolst et al, 2016). The predicted distribution (461+-72 m at 1 sigma) is wider than the distribution of observed librations (528+-31 m at 1 sigma) (Figure 10a). Thus librations put tighter bounds on the average crust thickness of Enceladus, although they do not constrain the other interior parameters. Enceladus' crust thickness varies mainly in latitude from 29+-4km at the equator (zonal average) to 14+-4 km and 7+-4 km at the north and south poles, respectively (Figure 11). Longitudinal variations are either subdominant, with crustal thickening along the tidal axis, or could be absent altogether as suggested by the latest estimates of the ellipsoidal shape. The very thin south polar crust facilitates the passage of water from the ocean to the surface and increases the concentration of tidal heating in the area. The variation in crust thickness could be due to crustal tidal heating which is indeed highest at the poles and lowest along the tidal axis.

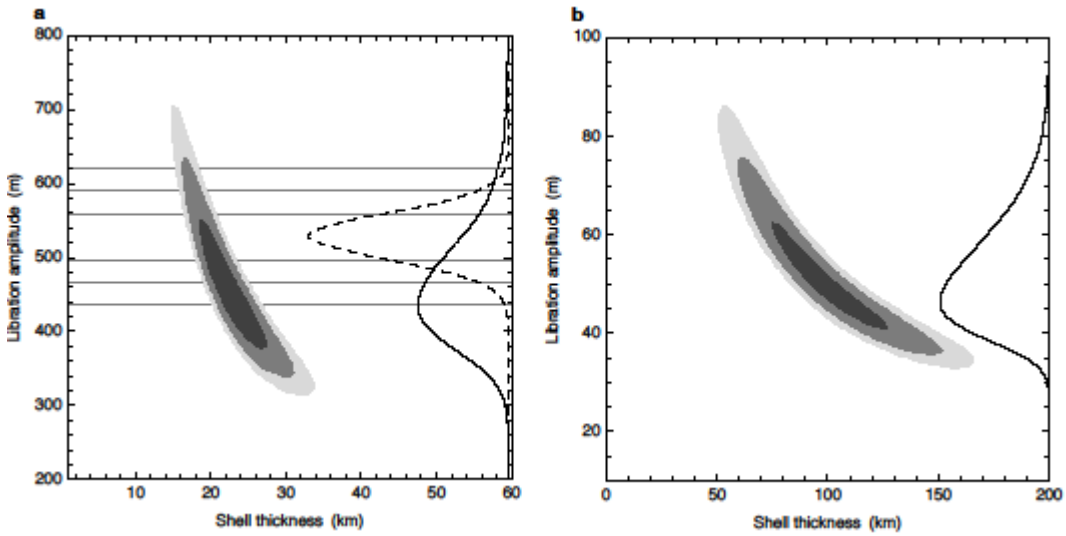

Figure 10: Libration amplitude: (a) Enceladus, (b) Dione. Contours show Bayesian confidence regions for models resulting from the gravity-shape inversion (1σ, 2σ, 3σ). Solid curves show the distributions of inferred librations. In panel (a), the dashed curve shows the distribution of observed librations (Thomas et al, 2016) with horizontal lines indicating the (1σ, 2σ, 3σ) ranges.

Comparison with librations can pinpoint data biases and constrain modelling choices. First, Enceladus' degree-three gravity favours a thinner crust than degree-two coefficients. Degree-two gravity however predicts a thinner crust (in agreement with librations) if the (degree 2, order 2) gravity coefficient is 2σ higher than the central value of the reference gravity solution SOL1, as suggested by the alternative gravity solution SOL2 (Iess et al, 2014). Alternatively, the degree-two shape could be responsible for the disagreement: while the new ellipsoidal shape of Thomas et al (2016} does not affect much the results, the recent ellipsoidal shape of Nadezhdina et al (2016) predicts more degree-two compensation and thus a thinner crust.

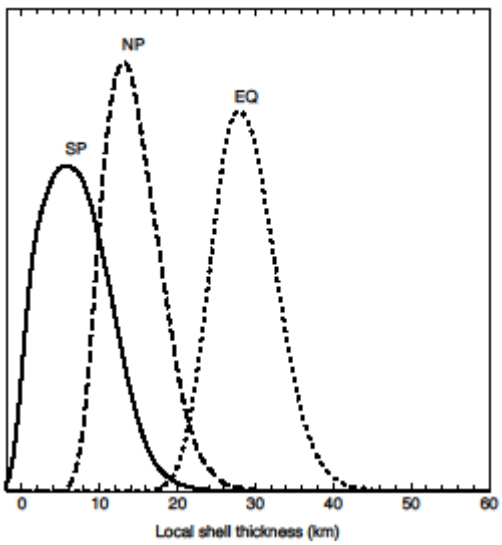

Figure 11: Local crust thickness of Enceladus. Solid, dashed, and dotted curves show the distributions of the inferred crust thickness at the south pole (SP), north pole (NP) and equator (EQ), respectively. The equatorial thickness represents the zonal average. Negative values are an artefact of histogram smoothing.

Second, we did not allow for a lot of surface porosity in our three-layer model, but we can easily do it with a four-layer model. The estimated crust thickness increases with porosity because surface topography contributes less to the gravity signal and must be less compensated. Consistency with librations suggests however that porosity is not an important factor. The average crustal stress is about 30 kPa for Enceladus, which is half of the average topographic stress, as expected in isostasy. It is comparable in magnitude to tidal stresses and could trigger the formation of the south polar terrain margins by gravitational spreading (Yin and Pappalardo, 2015). We also evaluated isostatic stresses in the core in order to check that they are always smaller than isostatic stresses in the crust. A final contentious point is that isostasy is only valid to first order in the flattening, contrary to the figure of equilibrium. The second-order error on the isostatic model, however, changes the total gravity potential by less than the data uncertainty.

In early 2016, Cassini gravity data became available for Dione (Figure 12), another satellite of Saturn which is in 2:1 orbital resonance with Enceladus (Hemingway et al, 2016). In comparison with Enceladus's case, classical Airy isostasy was even more problematic for Dione because it implied a 180 km thick icy crust that did not fit into the satellite, given the known size of the core. We thus decided to undertake the same isostatic analysis as for Enceladus. The inversion of shape and gravity and shape data yields a crust thickness of 99+-23 km (see Table I for the other parameters). Errors are much larger than for Enceladus (Figure 9) because of the large relative error on the shape. The gravity and shape data can thus be explained if there is a global ocean deep under the surface, whose past existence was already suggested by observation of ridge flexure (Hammond et al, 2013) and thermal history models (Multhaup et al, 2007).

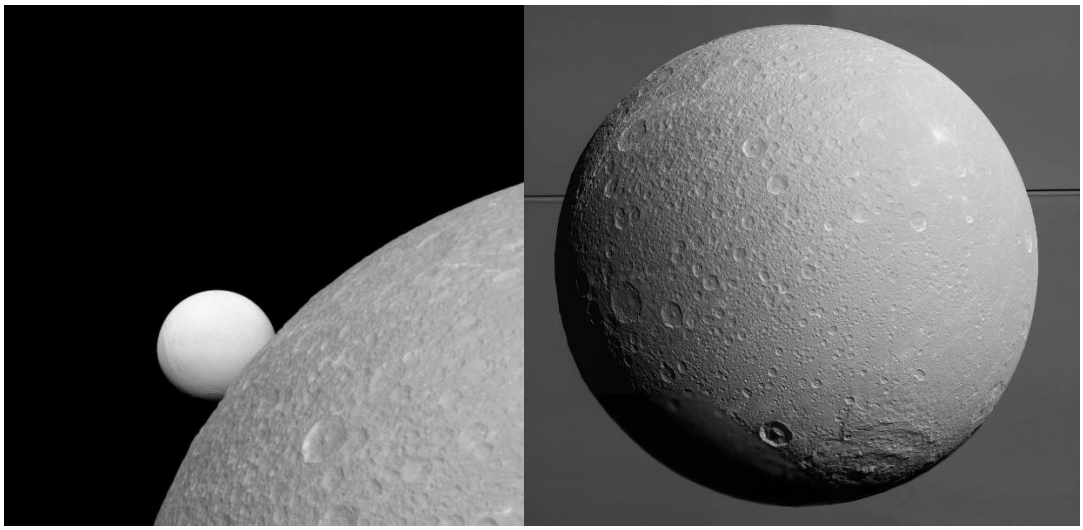

Figure 12: Left: Dione with Enceladus in the background, as viewed by Cassini on 8 September 2015. The surface of Enceladus is much brighter because of the constant rain of ice grains from its south polar jets (Image PIA18345). Right: Dione with Saturn and its rings in the background just prior to the Cassini's final close approach to the moon on 17 Augustus 2015. This picture illustrated the cover of the 16 October 2016 issue of Geophysical Research Letters in which our paper was published (Image PIA19650). Credit: NASA/JPL-Caltech/Space Science Institute.

We predict that Dione undergoes librations of amplitude 52+-10 m at 1 sigma (Figure 10b), one order of magnitude below Enceladus and thus not detectable in Cassini images but possibly in a future mission. Dione's crust thickness varies by less than five percent with a minimum at the poles and a maximum along the leading-trailing axis. Similarly to Enceladus, the zonal variation in crust thickness could be due to tidal heating, but we have no ready explanation for the longitudinal variation anticorrelated with tidal heating. Both satellites are more tectonized or resurfaced in their leading and trailing hemispheres than close to their tidal axis (Crow-Willard and Pappalardo, 2015; Kirchoff and Schenk, 2015).

Table I: Results of the Bayesian inversion of gravity-topography data for Enceladus and Dione.: mean values and 1 sigma Bayesian confidence intervals.

	Enceladus	Dione
Mean crust thickness (km)	23 ±4	99 ± 23
Mean ocean thickness (km)	38 ± 4	65 ± 30
Core radius (km)	192 ± 2	398 ± 14
Core density (kg/m3)	2422 ± 46	2435 ± 140

Dissipative ocean tides

Until now, dynamical ocean tides in icy satellites have been studied with the same Laplace Tidal Equations (LTE) that are used for Earth's tides (Tyler 2011; Chen et al, 2014; Matsuyama 2014; Hay and Matsuyama 2017). This model implies a surface ocean, making it impossible to assess how the crust damps resonant ocean tides. Crustal effects, however, are substantial in small and mid-size icy satellites. Using thin shell theory, we found that we could include crustal effects in the LTE with a method similar to the one we developed for the tidal coupling of a non-uniform thin shell: the crust is modelled as a thin massless shell whose effects on the ocean surface are quantified with pressure Love numbers. This approach has the advantage that the standard numerical and analytical methods for solving LTE remain applicable.

In the spectral domain, the LTE equations take the form of a truncated system of coupled linear equations which we solve with standard numerical methods. The LTE forcing term depends on the size and rheology of the crust and mantle, but mantle deformations are negligible for Enceladus. The most important crustal parameter is the membrane spring constant of the shell, which is proportional to the effective shear modulus of the viscoelastic crust and to the relative crust thickness. Crustal effects are generally substantial for Enceladus because the effective shear modulus of the crust is very large, in contrast with larger satellites such as Europa or Titan. Besides the full numerical solution, we derived simple scaling laws relating the surface and subsurface solutions for the resonances, the kinetic energy, and the dissipation rate (Figure 13). This scaling rule depends on the membrane spring constant of the crust and on oceanic self-attraction. The scaling rule works particularly well for bodies (such as Enceladus) whose ocean-to-bulk density ratio is close to 0.6.

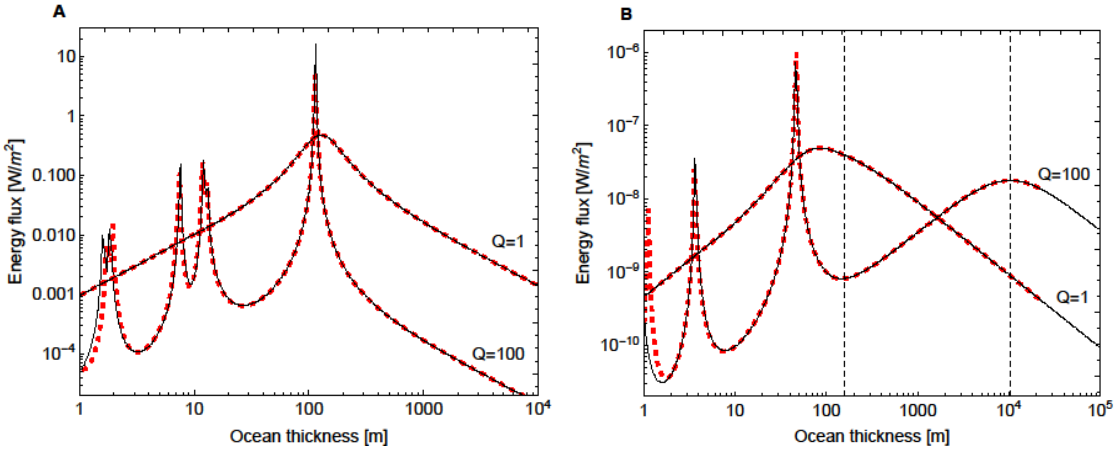

Figure 13: Oceanic dissipation if elastic crust: (A) eccentricity tides, (B) obliquity tides. The crust is 2.5 km thick. Dissipation results from linear top and bottom drag with either $Q = 100$ (moderate dissipation) or $Q = 1$ (very large dissipation). The surface energy flux is computed by solving the Laplace Tidal Equations for a subsurface ocean (solid curves). The dotted curves show the surface ocean solutions shifted by the presence of the crust. In panel B, the vertical dashed lines indicate where dissipation is maximum for the westward obliquity tide.

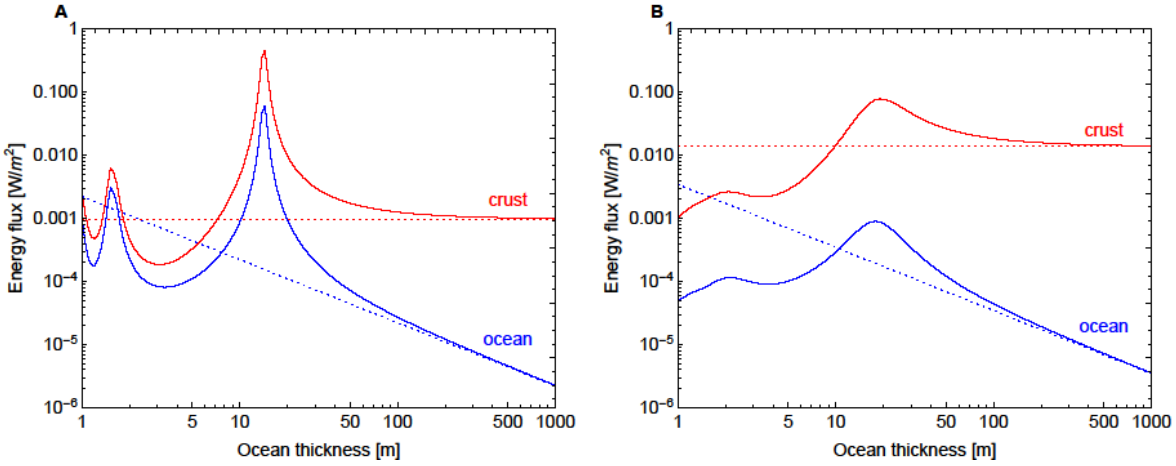

Figure 14: Dissipation in the crust and ocean due to eccentricity tides: (A) conductive crust, (B) convective crust. The contributions of crustal and oceanic dissipation to the surface energy flux are shown as separate curves. In each panel, the horizontal dotted line shows the deep-ocean asymptotic limit for crustal dissipation, whereas the oblique dotted line shows the deep-ocean asymptotic limit for oceanic dissipation.

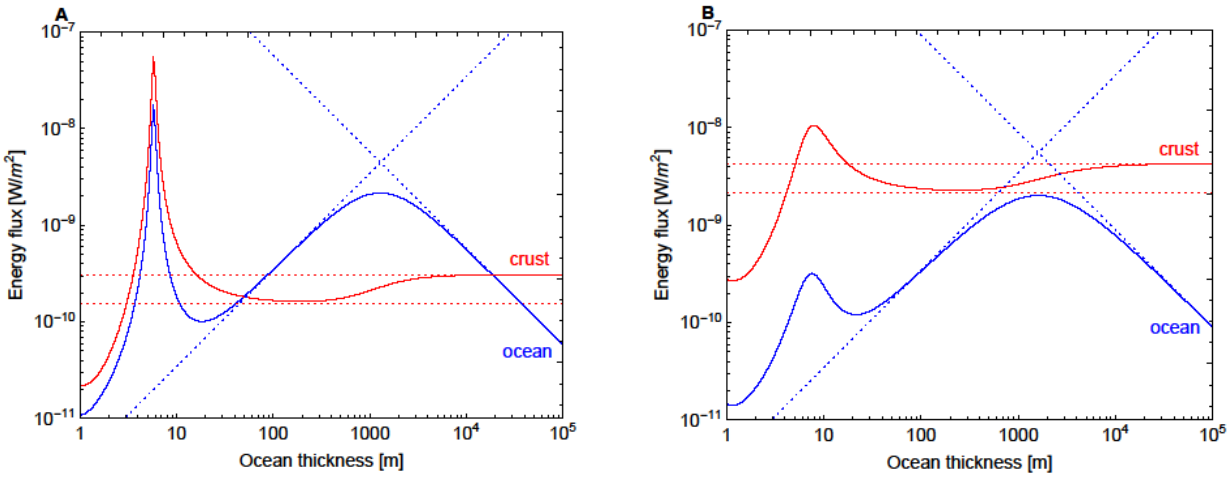

Figure 15: Dissipation in the crust and ocean due to obliquity tides: (A) conductive crust, (B) convective crust. The contributions of crustal and oceanic dissipation to the surface energy flux are shown as separate curves. In each panel, the horizontal dotted lines show the lower and upper bounds of the deep-ocean limit for crustal dissipation. The oblique dotted lines show the shallow- and deep-ocean asymptotic limits for oceanic dissipation due to the westward obliquity tide.

If the crust is elastic, tidal resonances are shifted to smaller ocean depths by a uniform scaling factor (Figure 13); the largest resonant depth is shifted from about 560 m to a few tens of meters (the exact value depends on the crust thickness and rigidity). If the crust is viscoelastic, tidal resonances are damped (in addition to being damped by ocean viscosity) and energy is dissipated in the crust (Figures 14 and 15). Resonances are shifted to smaller ocean depths as in the elastic case. For a shallow ocean, the dissipation rates in the crust and ocean exhibit the same resonances. For a deep ocean, crustal dissipation tends to a constant value (static tides) whereas oceanic dissipation tends to zero. The westward obliquity tide is a special case, because there is no radial tide unless the ocean is deep and the viscosity is high enough. Therefore, crustal dissipation due to dynamical obliquity tides can differ by up to a factor of two from the standard prediction assuming static tides (Figure 15). The same effect could play an important role for tectonics due to obliquity tides.

Crustal effects are thus severe for Enceladus' dynamical tides. If the crust is 25 km thick, resonances occur for an ocean less than 20 m deep, whereas the ocean depth is probably two or three orders of magnitude larger at the present time. Therefore, oceanic dissipation is nowadays negligible and crustal dissipation can be computed in the static limit. This conclusion can be avoided if the ocean is stratified, but it is doubtful that density stratification can be maintained if tidal heating occurs at the observed level. As regards obliquity tides, they exhibit interesting dynamical effects in deep oceans, but are way too small to be relevant to Enceladus unless future observations show that the obliquity is much larger than the theoretical upper bound for the Cassini state (Chen and Nimmo, 2011; Baland et al, 2016). In the past, tidal resonances could have played a role in a forming or freezing ocean less than 100 m deep. However, the displacement of resonances to very shallow depths compounds problems that already existed for a shallow surface ocean. First, the resonant response is blocked as soon as the deforming crust comes into contact with the mantle (or as the water dries out somewhere in a surface ocean). Second, the reliefs of the seafloor and `seaceiling' are comparable to the ocean depth and certainly alter the flow.

3. DISSEMINATION AND VALORISATION

Presentation of the results in seminars and international conferences

1. Beuthe, M., 2015. Localized bending and heating at Enceladus' south pole, European Planetary Science Congress, Nantes, France, 27 September-2 October 2015, Poster EPSC2015-524.
2. Beuthe, M., Rivoldini, A., Trinh, A., and Van Hoolst, T., 2015. Dynamical tides in icy satellites with subsurface oceans, European Planetary Science Congress, Nantes, France, 27 September-2 October 2015, Poster EPSC2015-479.
3. Beuthe, M., 2016. Enceladus's and Dione's floating ice shells, Seminar given at the Royal Observatory of Belgium, 8 November 2016.
4. Beuthe, M., 2016. Subsurface ocean tides in Enceladus and other icy moons, American Geophysical Union Fall Meeting 2016, San Francisco, USA, 12-16 December 2016, Poster P51B-2136.
5. Rivoldini, A., Beuthe M., Trinh A., 2016. What's the matter with Enceladus' gravity?, American Geophysical Union Fall Meeting 2016, San Francisco, USA, 12-16 December 2016, Poster P33A-2115.
6. Trinh, A., Rivoldini, A., Beuthe, M., Baland, R.-M., and Van Hoolst, T., 2016). The thickness of Enceladus' s ice shell as seen by Cassini, American Geophysical Union Fall Meeting 2016, San Francisco, USA, 12-16 December 2016, Poster P33A-2116.

Press releases of the Royal Observatory of Belgium

1. In French: http://www.astro.oma.be/fr/dione-une-lune-de-saturne-abrite-un-ocean-souterrain/
2. In Dutch: http://www.astro.oma.be/nl/saturnusmaan-dione-verbergt-een-oceaan-onder-het-ijs/
3. In English: http://www.astro.oma.be/en/saturns-moon-dione-harbors-a-subsurface-ocean/

Blogs

1. Feature on the blog of the American Geophysical Union (29 September 2016): http://blogs.agu.org/geospace/2016/09/29/research-suggests-saturns-moon-dione-may-harbor-subsurface-ocean/
2. Feature on the blog of the European Geophysical Union (20 December 2016): http://blogs.egu.eu/divisions/ps/2016/12/20/a-water-ocean-inside-saturns-moon-dione/

Interviews on the radio

1. Journal des Sciences de France Culture 14 October 2016:
http://media.radiofrance-podcast.net/podcast09/14312-14.10.2016-ITEMA_21104473-0.mp3
2. Emission "Sciences sans consciences…" de Radio Campus (interview de 45 mn),
15 November 2016:
http://public.radiocampus.be/161115_HDS_SE_Mikael_Beuthe_Satellites_de_Saturne.mp3

Written press

1. Article in Le Soir, 29 September 2016, Un océan souterrain découvert sur Saturne, based on a phone interview by Laetitia Theunis. Electronic link: http://www.lesoir.be/1329296/article/selection-abonnes/2016-09-29/un-ocean-souterrain-decouvert-sur-saturne
2. Articles in Metro, 29 September 2016, Un océan souterrain sur une lune de Saturne / Onder Saturnus bevindt zich 'Oceaanwereld', Electronic links: http://fr.metrotime.be/2016/09/29/must-read/un-ocean-souterrain-sur-une-lune-de-saturne/ and http://nl.metrotime.be/2016/09/29/must-read/oceaanwereld-onder-saturnus/
3. Highlight in Nature, 13 October 2016, Ocean on another of Saturn's moons, Electronic link: http://www.nature.com/nature/journal/v538/n7624/full/538143f.html

4. Article in Yale Scientific Magazine, 11 January 2017, Solid Evidence for Liquid Water on Dione, Electronic link: http://www.yalescientific.org/2017/01/solid-evidence-for-liquid-water-on-dione/

Electronic press
Many articles appeared in the press based on the joint press release of the Royal Observatory of Belgium and the blog of the American Geophysical Union. A non-exhaustive list for the international press (excluding the Belgian press) can be found at
https://wiley.altmetric.com/details/12267555/news
1. Article in Gizmodo, 30 September 2016, Another One of Saturn's Moons May Have a Global Ocean, based on a written interview by Maddie Stone, http://gizmodo.com/another-of-saturns-moons-may-have-a-global-ocean-1787275495
2. Article in Science, 4 October 2016, Subsurface ocean discovered on Saturn's moon Dione, http://www.sciencemag.org/news/sifter/subsurface-ocean-discovered-saturn-s-moon-dione
3. Article in Sky & Telescope, 10 October 2016, Does Dione have a subsurface ocean? by Camille Carlisle. http://www.skyandtelescope.com/astronomy-news/dione-subsurface-ocean-1010201623/
4. Article in in Flanders Today, 26 October 2016, Astronomers look for life beneath the surface of Saturn's moon, based on an interview by Leo Cendrowicz at the Royal Observatory. http://www.flanderstoday.eu/innovation/astronomers-look-life-beneath-surface-saturns-moon

Metrics
Impact of our paper Enceladus's and Dione's floating ice shells supported by minimum stress isostasy (according to Altmetric: https://wiley.altmetric.com/details/12267555):
- in the top 5% of all research outputs scored by Altmetric
- one of the highest-scoring outputs from this source (#10 of 8495)
- High Attention Score compared to outputs of the same age (99th percentile)
- High Attention Score compared to outputs of the same age and source (93rd percentile)
- mentioned by 67 news outlets, 8 blogs, 26 tweets, 5 Facebook pages
- The paper made the cover of the 16 October 2016 issue of Geophysical Research Letters in which it appeared (see Figure 12).

4. PERSPECTIVES

The non-uniform thin shell model will likely be an essential part of future models of tidal dissipation in Enceladus, whatever form they take. After the plunge in September 2017 of the Cassini spacecraft into Saturn, the next mission to the outer solar System will target Jupiter's moon Europa, whose water plumes recently made the headlines (Sparks et al, 2016; see also Roth et al, 2014). Non-uniform thin shell theory has thus a bright future at Europa. Finally, another promising field of application is studying the influence of non-uniform shell properties on the formation of tectonic features of icy moons.

Beyond Enceladus and Dione, our new take on isostasy is applicable to large icy satellites with global oceans, such as Europa (Nimmo et al, 2007), Titan (Nimmo and Bills, 2010), and particularly Ganymede whose gravity and shape will be measured by the European JUICE mission (Parisi et al, 2014). According to Park et al (2016), gravity and shape data from the Dawn mission suggest isostasy on Ceres, though the case is far from clear because compensation does not occur for all gravity components. Finally, isostasy plays a crucial role in understanding the long-wavelength gravity and shape as well as estimating the crust thickness of the planets Mars (Wieczorek and Zuber, 2004), Venus (James et al, 2013), and Mercury

(Perry et al, 2015). Thanks to the simultaneous availability of gravity/shape and libration data, Enceladus' case constitutes the first validation of planetary-scale isostasy.

Regarding dissipative tidal waves under an elastic crust, the approach coupling Laplace Tidal Equations to thin shell theory has been developed with maximum generality, so that it can easily be applied to other icy moons. Enceladus' crust is actually at the limit of validity of the membrane approach with its thickness just under ten percent of the surface radius. Crustal effects further increase when finite crust thickness is properly taken into account. However, no new physical effects are expected for ocean tides under a thick crust. The big question mark is rather the shallow water assumption. Is it a good approximation for subsurface oceans that are several tens (or even hundreds) of kilometres deep and which probably undergo mixing due to turbulent convection? Tidal flows in thick rotating shells exhibit complex features which are far from being understood. Ongoing research focuses on planetary fluid cores (under a very thick rigid shell) and on gaseous envelopes of giant planets and stars (with a free surface) (Ogilvie 2014; Le Bars et al, 2015). By contrast, large-scale dynamics of deep oceans under an elastic crust have received scant attention and are thus a promising field of research.

5. PUBLICATIONS

Peer reviewed

1. Beuthe, M., Rivoldini, A., and Trinh, A., 2016, Enceladus's and Dione's floating ice shells supported by minimum stress isostasy, Geophysical Research Letters 43, 10088-10096 (2016), doi:10.1002/2016GL070650, in open access on the e-print archive arXiv.org: arXiv:1610.00548
2. Beuthe, M., 2016, Crustal control of dissipative ocean tides in Enceladus and other icy moons, Icarus, 280, 278-299 (2016), doi:110.1016/j.icarus.2016.08.009, in open access on the e-print archive arXiv.org: arXiv:1608.08488

Others

5. Beuthe, M., 2015, Localized bending and heating at Enceladus' south pole, extended abstract for the European Planetary Science Congress 2015, available in electronic form: http://meetingorganizer.copernicus.org/EPSC2015/EPSC2015-524.pdf.
6. Beuthe, M., Rivoldini, A., Trinh, A., and Van Hoolst, T., 2015, Dynamical tides in icy satellites with subsurface oceans, extended abstract for the European Planetary Science Congress, 2015, available in electronic form:
http://meetingorganizer.copernicus.org/EPSC2015/EPSC2015-479.pdf
7. Beuthe, M., 2016. Subsurface ocean tides in Enceladus and other icy moons, American Geophysical Union Fall Meeting 2016, Poster P51B-2136 available in electronic form on AGU website: https://agu.confex.com/agu/fm16/meetingapp.cgi/Paper/135190
8. Beuthe, M., 2017, Localized tidal dissipation in Enceladus, ROB preprint, to be submitted to the peer-reviewed journal Icarus in April 2017. It will be immediately available in open access on the e-print archive arXiv.org

6. ACKNOWLEDGEMENTS

The research for the paper Enceladus's and Dione's floating ice shells supported by minimum stress isostasy was done in collaboration with A. Rivoldini and A. Trinh of the Royal Observatory of Belgium. A. Rivoldini is supported by the Belgian PRODEX program managed by the European Space Agency in collaboration with the Belgian Federal Science Policy Office. A. Trinh received support from the `Supplementary Researcher' programme managed by the Belgian Federal Science Policy Office, and from the European Research Council (ERC) under the European Union's Horizon 2020 research and innovation programme (grant agreement No 670874).

7. REFERENCES

Baland, R.-M., Yseboodt, M., and Van Hoolst, T., 2016. The obliquity of Enceladus, Icarus 268, 12-31.
Barr, A.C., 2008. Mobile lid convection beneath Enceladus' south polar terrain, J. Geophys. Res. 113, E07009, 1-14.
Barr, A.C., and McKinnon, W.B., Convection in Enceladus' ice shell: Conditions for initiation, Geophys. Res. Lett., 34, L09202, 1-6.
Beuthe, M., 2008. Thin elastic shells with variable thickness for lithospheric flexure of one-plate planets, Geophys. J. Int. 172, 817-841.
Beuthe, M., 2010. East-west faults due to planetary contraction, Icarus 209, 795-817.
Beuthe, M., 2013. Spatial patterns of tidal heating, Icarus 223, 308-329.
Beuthe, M., 2015a. Tides on Europa: the membrane paradigm, Icarus 248, 109-134.
Beuthe, M., 2015b. Tidal Love numbers of membrane worlds: Europa, Titan, and Co., Icarus 258, 239-266.
Beuthe, M., 2016. Crustal control of dissipative ocean tides in Enceladus and other icy moons, Icarus 280, 278-299.
Beuthe, M., Rivoldini, A., and Trinh, A., 2016. Enceladus's and Dione's floating ice shells supported by minimum stress isostasy, Geophys. Res. Lett. 43, 10088-10096.
Behounkova, M., Tobie, G., Choblet, G., and Cadek, O., 2010. Coupling mantle convection and tidal dissipation: Applications to Enceladus and Earth-like planets, J. Geophys. Res. 115, E09011, 1-20.
Behounkova, M., Tobie, G., Choblet, G., and Cadek, O., 2012. Tidally-induced melting events as the origin of south-pole activity on Enceladus, Icarus 219, 655-664.
Behounkova, M., Tobie, G., Choblet, G., and Cadek, O., 2013. Impact of tidal heating on the onset of convection in Enceladus's ice shell, Icarus 226, 898-904.
Behounkova, M., Tobie, G., Cadek, O., Choblet, G., Porco, C., and Nimmo, F., 2015. Timing of water plume eruptions on Enceladus explained by interior viscosity structure, Nat. Geosci. 8, 601-604.
Cadek, O., Tobie, G., Van Hoolst, T., Massé, M., Choblet, G., Lefèvre, A., Mitri., G., Baland, R.-M., Behounkova, M., Bourgeois, O., and Trinh, A., 2016, Enceladus's internal ocean and ice shell constrained from Cassini gravity, shape, and libration data, Geophys. Res. Lett. 43, 5653-5660.
Chen, E.M.A. and Nimmo, F., 2011. Obliquity tides do not significantly heat Enceladus, Icarus 214, 779-781.
Chen, E.M.A., Nimmo, F., and Glatzmaier, G.A., 2014, Tidal heating in icy satellite oceans, Icarus 229, 11-30.
Collins, G.C., and Goodman, J.C., 2007. Enceladus' south polar sea, Icarus 189, 72-82.

Crow-Willard, E.N., and Pappalardo, R.T., 2015, Structural mapping of Enceladus and implications for formation of tectonized regions, J. Geophys. Res. 120, 928-950.
Dahlen F.A., 1982, Isostatic geoid anomalies on a sphere, J. Geophys. Res. 87, 3943-3947.
Greff-Lefftz, M., Métivier, L., and Besse, J., 2010. Dynamic mantle density heterogeneities and global geodetic observables, Geophys. J. Int. 180, 1080-1094.
Gregory, P. C., 2005. Bayesian Logical Data Analysis for the Physical Sciences, Cambridge University Press, Cambridge.
Hammond, N.P., Phillips, C.B., Nimmo, F., and Kattenhorn, S.A., 2013. Flexure on Dione: Investigating subsurface structure and thermal history, Icarus 223, 418-422.
Han, L. Tobie, G., and Showman, A.P., 2012. The impact of a weak south pole on thermal convection in Enceladus' ice shell, Icarus 218, 320-330.
Hay, H., and Matsuyama, I., 2017, Numerically modelling tidal dissipation with bottom drag in the oceans of Titan and Enceladus, Icarus 281, 342-356.
Hedman, M. M., Gosmeyer, C.M., Nicholson, P.D., Sotin, C., Brown, R.H., Clark, R.N., Baines, K.H., Buratti, B.J., and Showalter, M.R., 2013. An observed correlation between plume activity and tidal stresses on Enceladus, Nature 500, 182-184.
Hemingway, D.J., Zannoni, M., Tortora, P., Nimmo, F., Asmar, S.W., 2016. Dione's internal structure inferred from Cassini gravity and topography, Lunar and Planetary Science Conference 47, abstract 1314.
Howett, C.J.A, Spencer, J., Pearl, J., and Segura, M., 2011. High heat flow from Enceladus' south polar region measured using 10-600 cm-1 Cassini/CIRS data, J. Geophys. Res. 116, E03003, 1-15.
Hsu, H.-W., Postberg, F., Sekine, Y., Shibuya, T., Kempf, S., Horanyi, M., Juhasz, A., Altobelli, N., Suzuki, K., Masaki, Y., Kuwatani, T., Tachibana, S., Sirono, S.-I., Moragas-Klostermeyer, G., and Srama, R., 2015. Nature 207, 207-210.
Hurford, T. A. Helfenstein, P., Hoppa, G.V., Greenberg, R., and Bills, B.G., 2007. Eruptions arising from tidally controlled periodic openings of rifts on Enceladus, Nature 447, 292-294.
Iess, L. Stevenson, D.J., Parisi, M., Hemingway, D., Jacobson, R.A., Lunine, J.I., Nimmo, F., Armstrong, J.W., Asmar, A.W., Ducci, M., and Tortora, P., 2014. The gravity field and interior structure of Enceladus, Science 344, 78-80.
James, P.B., Zuber, M.T., and Phillips, R.J., 2013. Crustal thickness and support of topography on Venus, J. Geophys. Res. 118, 859–875.
Jeffreys, H., 1970. The Earth, Cambridge Univ. Press, Cambridge, U.K.
Kirchoff, M.R., and Schenk, P., 2015. Dione's resurfacing history as determined from a global impact crater database, Icarus 256, 78-89.
Kirk, R.L., and Stevenson, D.J., 1987. Thermal evolution of a differentiated Ganymede and implications for surface features, Icarus 69, 91-134.
Lainey, V., Karatekin, O., Desmars, J., Charnoz, S., Arlot, J.-E., Emelyanov, N., Le Poncin-Lafitte, C., Mathis, S., Remus, F., Tobie, G., and Zahn, J.-P., 2012. Strong tidal dissipation in Saturn and constraints on Enceladus' thermal state from astrometry, Astrophys. J. 752, 14, 1-19.
Lainey, V., Jacobson, R.A., Tajeddine, R., Cooper, N.J., Murray, C., Robert, V., Tobie, G., Guillot, T., Mathis, S., Remus, F., Desmars, J., Arlot, J.-E., De Cuyper, J.-P., Dehant, V., Pascu, D., Thuillot, W., Le Poncin-Lafitte, C., and Zahn, J.-P., 2017. Icarus 281, 286-296.
Lambeck, K., 1988. Geophysical Geodesy, Clarendon Press, Oxford, U.K.
Le Bars, M., Cébron, D., and Le Gal, P., 2015. Flows driven by libration, precession, and tides, Ann. Rev. Fluid Mech., 47, 163-193.
Malamud, U. and Prialnik, D., 2013. Modeling serpentinization: Applied to the early evolution of Enceladus and Mimas, Icarus 225, 763-774.
Matsuyama, I., 2014. Tidal dissipation in the oceans of icy satellites, Icarus 242, 11-18.
McCarthy, C., and Cooper, R.F., 2016, Tidal dissipation in creeping ice and the thermal evolution of Europa, Earth Planet. Sci. Lett. 443, 185-194.
McKinnon, W.B., 2013. The shape of Enceladus as explained by an irregular core: Implications for gravity, libration, and survival of its subsurface ocean, J. Geophys. Res. 118, 1775-1788.

McKinnon, W.B., 2015. Effect of Enceladus's rapid synchronous spin on interpretation of Cassini gravity, Geophys. Res. Lett., 42, 2137-2143.
Meyer, J. and Wisdom, J., 2007. Tidal heating in Enceladus, Icarus 188, 535-539.
Mitri, G., and Showman, A.P., 2008. Thermal convection in ice-I shells of Titan and Enceladus, Icarus 193, 387-396.
Multhaup, K., and Spohn, T., 2007. Stagnant lid convection in the mid-sized icy satellites of Saturn, Icarus, 186, 420–435.
Nadezhdina, I.E. Zubarev, A.E., Brusnikin, E.S., and Oberst, J., 2016. A libration model for Enceladus based on geodetic control point network analysis, Int. Arch. Photogramm. Remote Sens. Spatial Inf. Sci., XLI-B4, 459–462.
Nimmo, F. Spencer, J.R., Pappalardo, R.T., and Mullen, M.E., 2007. Shear heating as the origin of the plumes and heat flux on Enceladus, Nature 447, 289-291.
Nimmo, F., and Bills, B.G., 2010. Shell thickness variations and the long-wavelength topography of Titan, Icarus, 208, 896–904.
Nimmo, F., Bills, B.G., and Thomas, P.C., 2011, Geophysical implications of the long-wavelength topography of the Saturnian satellites, J. Geophys. Res. 116, E11001, 1-12.
Nimmo, F., Porco, C., and Mitchell, C., 2014. Tidally modulated eruptions on Enceladus: Cassini ISS observations and models, Astron. J. 148, 46.
Ogilvie, G.I., 2014. Tidal dissipation in stars and giant planets, Ann. Rev. Astr. Astrophys., 52, 171-210.
O'Neill, C., and Nimmo, F., 2010. The role of episodic overturn in generating the surface geology and heat flow on Enceladus, Nat. Geosci. 88-91.
Parisi, M., Iess, I., Finocchiaro, S., 2014, The gravity fields of Ganymede, Callisto and Europa: how well can JUICE do?, European Geophysical Union Assembly 2014, abstract EGU2014-11758.
Park, R.S., Konopliv, A.S., Bills, B., Rambaux, N., Castillo-Rogez, J., Raymond, C.A., Vaughan, A.T., Ermakov, A., Zuber, M.T., Fu, R.R., Toplis, M.J., Russell, C.T., Nathues, A. and Preusker, F.,2016. A partially differentiated interior for (1) Ceres deduced from its gravity field and shape, Nature, 537, 515–517.
Perry, M.E., Neumann, G.A., Phillips, R.J., Barnouin, O.S., Ernst, C.M., Kahan, D.S., Solomon, S.C., Zuber, M.T., Smith, D.E., Hauck II, S.A., Peale, S.J., Margot, J.-L., Mazarico, E., Johnson, C.J., Gaskell, R.W., Roberts, J.H., McNutt Jr, R.L., and Oberst, J., 2015. The low-degree shape of Mercury, Geophys. Res. Lett., 42, 6951-6958.
Porco, C.C., Helfenstein., P., Thomas, P.C., Ingersoll, A.P., Wisdom, J., West, R., Neukum, G., Denk, T., Wagner, R., Roatsch, T., Kieffer, S., Turtle, E., McEwen, A., Johnson, T.V., Rathbun, J., Veverka, J., Wilson, D., Perry, J., Spitale, J., Brahic., A., Burns, J.A., DelGenio, A.D., Dones, L., Murray, C.D., and Squyres, S., 2006. Cassini observes the active south pole of Enceladus, Science 311, 1393-1401.
Porco, C.C. DiNino, D., and Nimmo, F., 2014. How the geysers, tidal stresses, and thermal emission across the South Polar Terrain of Enceladus are related, Astron. J. 148, 45.
Postberg, F. Kempf, S., Schmidt, J., Brilliantov, N., Beinsein, A., Abel, B., Buck, U., and Srama, R., 2009. Sodium salts in E-ring ice grains from an ocean below the surface of Enceladus, Nature 459, 1098-1101.
Postberg, F. Schmidt, J., Hillier, J., Kempf, S., and Srama, R., 2011. A salt-water reservoir as the source of a compositionally stratified plume on Enceladus, Nature 474, 620-622.
Roberts, J., 2014. The fluffy core of Enceladus, Icarus 258, 54-66.
Roberts, J. and Nimmo, F., 2008. Tidal heating and the long-term stability of a subsurface ocean on Enceladus, Icarus 194, 675-689.
Ross, M. N. and Schubert, G., 1989. Viscoelastic models of tidal heating in Enceladus, Icarus 78, 90-101.
Roth, L., Saur, J., Retherford, K.D., Strobel, D.F., Feldman, P.D., McGrath, M.A., Nimmo F., 2014. Transient water vapor at Europa's south pole, Science 343, 171-174.

Rozel, A., Besserer, J., Golabek, G.J., Kaplan, M., and Tackley, P.J, 2014. Self-consistent generation of single-plume state for Enceladus using non-Newtonian rheology, J. Geophys. Res. 119, 416-439.
Rudolph, M.L., and Manga, M., 2009. Fracture penetration in planetary ice shells, Icarus 199, 536-541.
Sabadini, R., and Vermeersen, B., 2004. Global Dynamics of the Earth, Kluwer Acad., Dordrecht, Netherlands.
Sambridge, M., and Gallagher, K., 2011. Inverse Theory, Monte Carlo Method, in Encyclopedia of Solid Earth Geophysics, edited by H. K. Gupta, pp. 639–644, Springer Netherlands, Dordrecht.
Shampine, L.F., Muir, P.H., and Xu, H., 2006. A user-friendly Fortran BVP solver, J. Num. Anal. Ind. Appl. Math., 1(2), 201–217.
Shoji, D., Hussmann, H., Kurita, K., and Sohl, F., 2013. Ice rheology and tidal heating of Enceladus, Icarus 226, 10-19.
Shoji, D. Hussmann, H., Kurita, K., and Sohl, F., 2014. Non-steady state tidal heating of Enceladus, Icarus 235, 75-85.
Spahn, F., Schmidt, J., Albers, N., Hörning, M., Makuch, M., Seiß, M, Kempf, S., Srama, R., Dikarev, V., Helfert, S., Moragas-Klostermeyer, G., Krivov, A.V., Sremcevic, M., Tuzzolino, A.J., Economou, and T., Grün E., 2006. Cassini Dust Measurements at Enceladus and implications for the origin of the E ring, Science 311, 1416-1418.
Sparks, W.B. , Hand, K.P., McGrath M.A., Bergeron E., Cracraft M., and Deustua S.E., 2016. Probing for evidence of plumes on Europa with HST/STIS, Astr. J. 829, 121.
Spencer, J. R, Pearl, J.C., Segura, M., Flasar, F.M., Mamoutkine, A., Romani, P., Buratti, B.J., Hendrix, A.R., Spilker, L.J., and Lopes, R.M., 2006. Cassini encounters Enceladus: background and the discovery of a south polar hot spot, Science 311, 1401-1405.
Spencer, J.R., Howett, C.J.A., Verbiscer, A., Hurford, T.A., Segura, M., and Spencer, D.C., 2013. Enceladus Heat Flow from High Spatial Resolution Thermal Emission Observations, European Planetary Science Congress 2013, abstract EPSC2013-840-1.
Spencer, J.R., Howett, C.J.A., Verbiscer, A., Hurford, T.A., and Gorius, N.J.P., 2016. High resolution observations of active and passive thermal emission from Enceladus' south pole in 2015: the closest and the coldest, Lunar and Planetary Science Conference 47, abstract 2860.
Spitale, J.N., and Porco, C., 2007. Association of the jets of Enceladus with the warmest regions on its south-polar fractures, Nature 449, 695-697.
Thomas, P.C., Tajeddine, R., Tiscareno, M.S., Burns, J.A., Joseph, J., Loredo, T.J., Helfenstein, P., and Porco, C., 2016. Enceladus's measured physical libration requires a global subsurface ocean, Icarus 264, 37-47.
Tobie, G, Cadek, O., and Sotin, C., 2008. Solid tidal friction above a liquid water reservoir as the origin of the south pole hotspot on Enceladus, Icarus 196, 642-652.
Travis, B.J., and Schubert, G., 2015. Keeping Enceladus warm, Icarus 250, 32-42.
Tyler, R., 2011. Tidal dynamical considerations constrain the state of an ocean on Enceladus, Icarus 211, 779-779.
Tyler, R., 2014. Comparative estimates of the heat generated by ocean tides on icy satellites in the outer Solar System, Icarus 243, 358-385.
Van Hoolst, T., Baland, R.-M., and Trinh, A., 2016. The diurnal libration and interior structure of Enceladus, Icarus 277, 311-318.
Waite, J. H. Lewis, W.S., Magee, B.A., Lunine, J.I., McKinnon, W.B., Glein, C.R., Mousis, O., Young, D.T., Brockwell, T., Westlake, J., Nguyen, M.-J., Teolis, B.D., Niemann, H.B., McNutt, R.L., Perry, M., and Ip, W.-H., 2009. Liquid water on Enceladus from observations of ammonia and Ar in the plume, Nature 460, 487-490.
Wieczorek, M.A., and Zuber, M.T., 2004. Thickness of the Martian crust: Improved constraints from geoid-to-topography ratios, J. Geophys. Res., 109, E01009.
Wieczorek, M.A., Meschede, M., Oshchepkov, I., Sales de Andrade, E., and heroxbd, 2016. SHTOOLS: Version 4.0., Zenodo, doi:10.5281/zenodo.206114

Yin, A., and Pappalardo, R.T., 2015. Gravitational spreading, bookshelf faulting, and tectonic evolution of the South Polar Terrain of Saturn's moon Enceladus, Icarus, 260, 409–439.